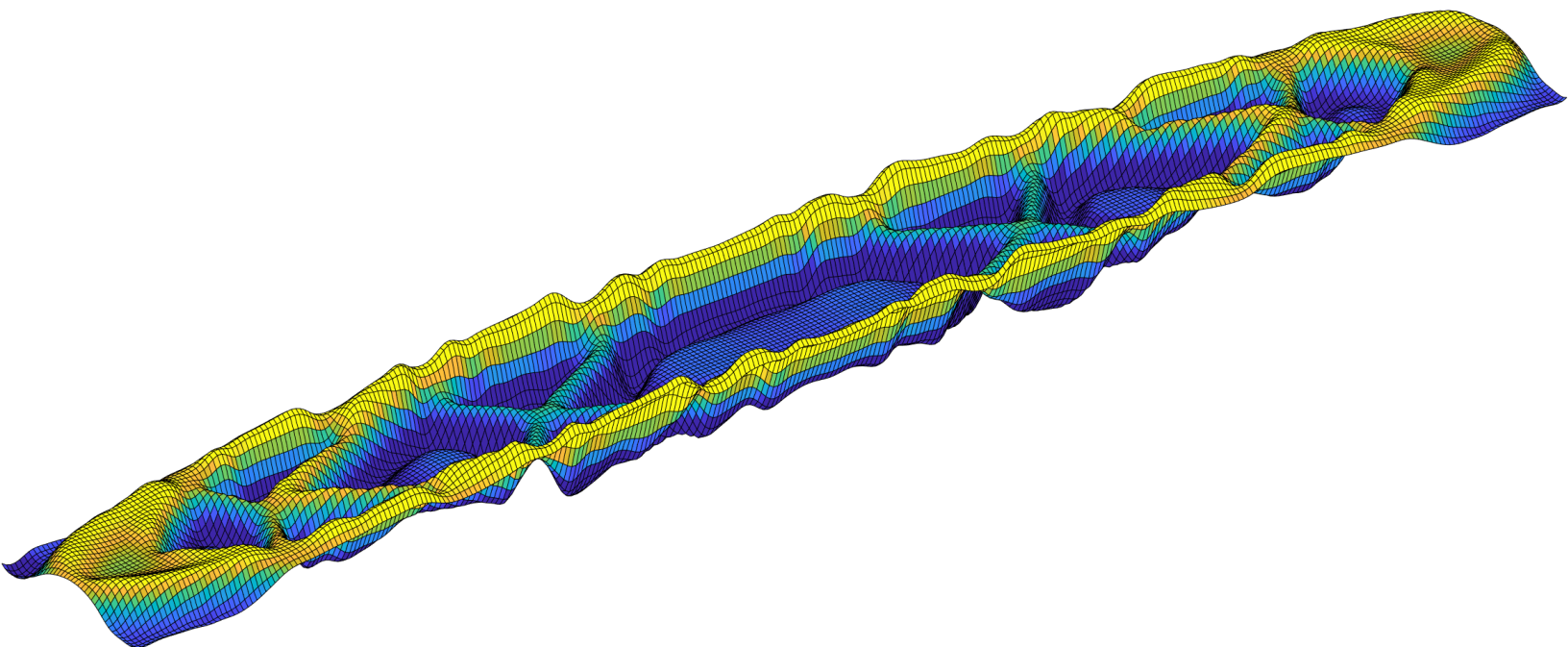# Department of Precision and Microsystems Engineering

Density and level-set based topology optimization for structural vibration problems: A comparative study

Julius Keur

Report no	: 2022.069
Coach	: Lise Noël, Tom van Adrichem
Professor	: Matthijs Langelaar
Specialisation	: Structural optimization mechanics
Type of report	: Master thesis
Date	: November 4, 2022

TU Delft
Delft
University of
Technology

Precision and Microsystems Engineering

Challenge the future

Density and level-set based topology optimization for structural vibration problems: A comparative study

Master Thesis

by

Julius Keur

to obtain the degree of Master of Science
at the Delft University of Technology,
to be defended publicly on Friday November 4, 2022 at 10:00 AM.

Student number:	4342879
Project duration:	September 6, 2021 – November 4, 2022
Thesis committee:	Dr. Ir. M. Langelaar, TU Delft
	Dr. Ir. L. F. P. Noël, TU Delft
	Dr. Ir. A. M. Aragón, TU Delft
	Ir. T. van Adrichem, Demcon

Abstract

High performance machines rely on fast moving parts and generally avoid resonance for improved accuracy. To improve the dynamic properties of these high performance machines, their parts are optimized via a lengthy iterative process. Topology optimization for vibrations problems could shorten this time consuming design process and provide a more optimal design compared to the manual iteration process.

In the field of topology optimization for vibration problems there are various methods to solve a given problem. The two most commonly used methods in recent research are the density approach and the level-set approach. The characteristics of the density and level-set approach are well understood in context of topology optimization for vibration problems, however a direct comparison between these two methods has not yet been conducted. Several crucial aspects of topology optimization for vibration problems will be investigated, such as localized eigenmodes, mode multiplicity, grey areas and efficiency for practical applications. Additionally, the applicability of these aspects will be tested in the academic and industrial field to determine their values when applied in industry. This thesis provides an extensive study of various design cases in which the density and level-set topology optimization approaches are compared on their ability to solve vibration problems. These design cases are based on frequently used design cases in literature which are generally seen as benchmark problems.

For this thesis it is opted to have as many similarities between the density and level-set approach as possible, to ensure a fair comparison between the two methods. To accomplish this, the level-set approach uses a density based mapping in combination with material parameter sensitivities and the method of moving asymptotes (MMA) to update the design variables. Furthermore, the level-set function is parameterized with compactly supported radial basis functions (CSRBF). This leaves the difference that the density approach uses element densities as design variables, whereas the level-set approach uses expansion coefficients as design variables.

The design cases indicate that the density approach is versatile as it is able to solve a wide variety of problems. Additionally, there are less parameters, which makes this method easier and faster to work within an industrial setting. Furthermore, the method produces well-performing designs even with more difficult tasks, such as a coarse mesh. Although occasionally localized eigenmodes occurred whilst using this method, they do not seem to interfere with the final result. Thus, the density approach is less time consuming to setup and needs less tuning of the method specific parameters. On the other hand, results from the design cases also indicated that the level-set approach is able to produce designs with an improved objective function at the cost of possibly more tuning of method specific parameters. Furthermore, the level-set approach is able to solve all the design cases without the occurrence of localized eigenmodes. Although the level-set approach is less optimal for coarse meshes, it outperforms the density approach at more refined mesh sizes. Additionally, it features a crisp geometry description by the zero level-set contour. Thus, the level-set approach is able to produce more optimal designs without the occurrence of local eigenmodes at the cost of more complexity and possibly more tuning of the method specific parameters.

To conclude, both approaches have unique properties to be able to solve vibration problems. The density approach is more applicable as a standard approach in an industrial setting due to it being more robust and the method is less time consuming. However, the level-set approach should be opted for more complex vibration problems due to the crisp geometry definition of complex geometric features and its ability to outperform the density approach. A practical application has been solved with an optimization run, where the use of a set of predefined parameters that solved the benchmark cases has been used. Additionally, an optimization run where all parameters are optimized for the specific design case was performed to see the ultimate performance. The level-set approach was able to outperform the density approach in the predefined parameter case, whereas the ultimate performance case gave usable results for both methods. The differences came down to a more improved objective function for the density approach, or a more simplistic and lighter design for the level-set approach.

Preface

"There is no elevator to success, you have to take the stairs" – Zig Ziglar

This quote describes my experience in the process of a year's worth of work, which is put together in a 63 page thesis that ultimately got my master degree. It was not always easy and there were lots of ups and downs. However, in the end, when you look down the stairs, you can see how many big steps I have taken and that the end result is something to be very proud of.

I would like to thank Demcon and the Precision and Microsystems Engineering department at the TU Delft for the collaboration and providing me with the opportunity for my graduation project. The topic gave me a lot of insight in the world of topology optimization, which is a wonderful tool to solve engineering problems.

My gratitude goes to my supervisor Tom van Adrichem from Demcon. He was there to mentor me and helped me develop my hard and soft skills. The sincere interest in the topic, even though it was sometimes hard to comprehend, was very gratifying. Not only the formal conversations were helpful, but the small talk was very entertaining as well. Also, staying in touch while he was leaving for a different company gave me a lot of joy and motivation to continue the project.
Furthermore, I would like to thank Lise Noël for the diligent support, helping me out for the in-depth technical questions and reading my somewhat unpleasant drafts. Even though my questions were sometimes difficult to explain over the Zoom meetings, she was always helpful to solve my problems. Next to that I would like to thank Matthijs Langelaar for providing me with valuable feedback.
Of course my parents, who have been supportive and whom I could amaze with the intricacy of my thesis. And finally Veerle, who spent an unhealthy amount of time proof-reading my drafts, teaching me how to write properly, was very supportive and helped me staying motivated throughout the year.
Thank you.

Julius Q. Keur
Delft, September 2022

Contents

1   Introduction

In many engineering problems, the attenuation of vibration, noise and dynamic responses is a major concern. In the field of ultra-precision systems the position tolerances are within the nanometer magnitudes, while the movement speed and acceleration can be up to 1 m/s and 40 m/s^2 respectively. Such a system can be seen in Figure 2. To obtain these high speed movements these systems must have a lightweight construction. Such lightweight constructions have an inherent drawback: they lead to an increase in high frequency disturbances. These disturbances are difficult to cancel out by design or active control. For lightweight systems the controller and actuator bandwidth need to work at considerable high frequencies [Wang et al., 2019]. This is either costly or impossible to implement. Therefore, the interest of this industry in structures optimized for vibrations is continously increasing.

1.1   Problem formulation

Another field of application is making lighter electronic systems, such as portable electronic devices, micro-electro-mechanical systems or implanted electronic devices. These devices rely on vibrations in a specific range for their application. These vibrations will be applied via an actuator and a spring. Advances in technology have resulted in smaller batteries and actuators, however more gains can be made by tuning the spring for the specified application. A practical application of such a design case is the Chest Master, which is a medical device used to treat patients with cystic fibrosis in the lungs. The Chest Master uses vibrations to clear up mucus that builds up in the lungs. From experimental data it is found that a frequency of 12.5 Hz results in removal of the mucus in the lungs. A challenge from this device is that multiple actuators need to be placed around the patients chest for a prolonged period of time. These actuators are heavy and consume a considerable amount of energy. To make the system more energy efficient, it is wished that the spring of the actuator resonates at the same eigenfrequency as the operating eigenfrequency. This in turn results in less power input for the actuators and consequently a smaller and lighter device. An example of this device is shown in Figure 3.

General methods to achieve such a specific frequency would be to produce geometric shapes in a trial and error process or perform a size or shape optimization. The problem with a trial and error process is that there
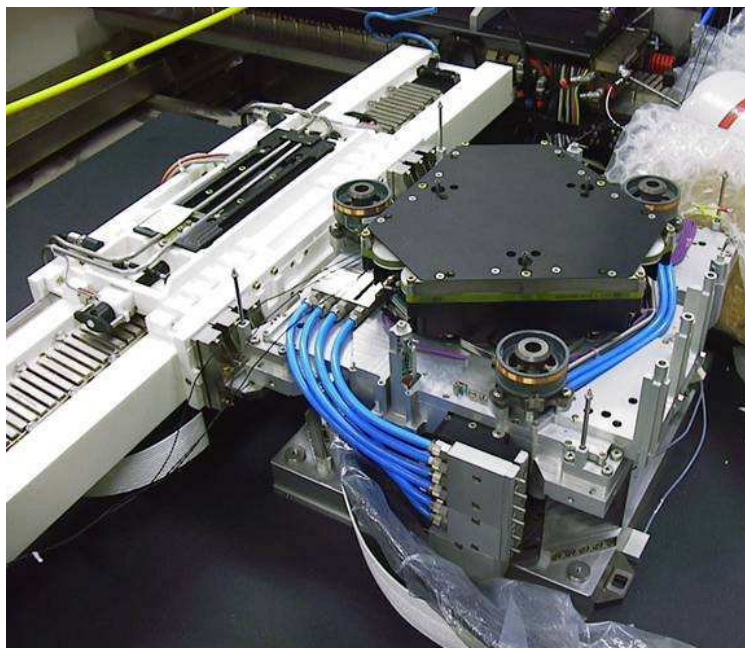

Figure 2: Wafer positioning system that needs to avoid resonance for accurate positioning [Heertjes and Vardar, 2013].

Figure 3: Chest Master suit for cystic fibrosis patients [de Vlieger, 2014]

is no systematic improvement towards the eigenfrequency of interest. This holds especially when dealing with optimizing a structure for its eigenfrequency, where it is difficult to realize design improvements due to the complexity of the physics. Furthermore, the difficulty of size and shape optimization is that the results are highly dependent on the initial inputs. As eigenfrequency optimization is a non-linear optimization process, it makes solving such a design case even harder.

1.2 Topology optimization

A solution to such a problem would be to optimize the given geometry via the use of topology optimization. Topology optimization is a methodical approach which gives the possibility to achieve a solution to such a specific design case. One of the first methods presented to solve vibration problems in topology optimization was proposed by Ma et al. [1993], where a frequency response problem of a vibrating structure is solved via the homogenization method. In a work of Pedersen [2000] the density approach was proposed to solve a vibration problem. Via the use of a slight variation of the solid isotropic material with penalization (SIMP) model he maximized eigenvalues various design cases. A few years later Allaire and Jouve [2005] proposed one of the first level-set approaches to solve topology optimization for vibration problems. A density based mapping with the Hamilton-Jacobi update scheme was used. From here on the level-set approach is applied in various forms to solve vibration problems with topology optimization. Nowadays, the density and level-set approach are one of the most used methods to solve structural optimization problems for vibrations.

A well-known effect that results from the use of topology optimization in vibration problems is that the computation time is a substantial burden. Moreover, sensitivity information at multiplicity and preventing the occurrence of localized eigenmodes are common problems that need to be solved.

First of all, there are several solutions to reduce the computational burden of eigenvalues. They can be listed as: model reduction schemes Li et al. [2021a], multi-level solution methods (also referred to as multi-resolution or multi-grid) [Amir et al., 2014] and element removal methods as seen in Behrou et al. [2021] all prove to be efficient techniques to reduce computation time.

Furthermore, sensitivity information of eigenvalues at multiplicity tends to be problematic, as the sensitivity information is non-unique. A method to distinguish the sensitivities at multiplicity is proposed by Seyranian

et al. [1994] and later implemented by Du and Olhoff [2007].

Localized modes are a consequence due to the existence of low density areas. These low density areas are very flexible and thus control the lowest eigenmodes of the system. In a vibration finite element method (FEM) analysis a set of eigenfrequencies are calculated to obtain the desired eigenfrequency range. When low eigenfrequencies with mode shapes in the low density regions occur, they reduce the range of the structurally relevant eigenfrequencies. There are various methods to handle such localized eigenmodes, for example by removing elements [Yoon, 2010] or using a density approach that prevents a zero gradient of the elements [Sigmund and Maute, 2013].

As topology optimization becomes more readily available in commercial finite element packages, there is a rising interest into the possibilities of the available methods. Not only the possibilities are of interest, but also the problems that can occur during an optimization run. A comparison between the most popular methods and possible design cases could provide a basis for a guideline to make the tool more accessible to the industry.

1.3   Comparisons in literature

The main objective of this thesis is to provide a comprehensive review of topology optimization problems for vibrating structures, where the density based approach and level-set based approach are compared to one another. Several past articles have focused on aspects of this topic. Rozvany [2009] provided a review of the use of topology optimization in commercial software packages. The SIMP and evolutionary structural optimization (ESO) methods have been compared to one another. The overall conclusion was that the SIMP method is able to provide a solution near the global minimum for originally convex optimization problems. However, SIMP is used in practise for highly non-convex optimization problems, therefore a global minimum cannot be guaranteed. Furthermore, the ESO method is depicted as heuristic, computationally inefficient, occasionally unreliable and chaotic. In Sigmund and Maute [2013] an overview, comparison and critical review of different approaches, similarities, weaknesses, strengths and guidelines of topology optimization is presented. The overall conclusion from this work was that all the available approaches have similar performances and the nuances lie in the efficiency, general applicability, constraints, boundary conditions, independence on starting guess, tuning parameters, mesh-independent convergence and ease of use. Furthermore, Villanueva and Maute [2014] employed a practical comparison between the density and level-set approaches. The two methods are compared to one another in 3D design cases with a compliance optimization objective. They concluded that the implemented level-set approach describes the geometry with a crisp result and an acceptable accuracy even on a coarse mesh. Another practical comparison of the density, ESO and level-set methods from Dilgen et al. [2019] compares these methods for acoustic mechanical interaction problems. It was found that the density-based approach resulted in the highest performing designs. However, the level-set approach is favored due to the complex multi-physical nature of the optimization problem, as the level-set method solves these physics problems with more ease. A lack of a good continuation scheme in the level-set method resulted in poorer local minima compared to the density method. Finally, Zargham et al. [2016] presented a comparative review of established literature of topology optimization problems for structural designs under vibration problems.

1.3.1   Motivation and goals

Although the characteristics of the density and level-set methods are well understood in context of topology optimization for vibration problems, a direct comparison between these two methods has not yet been conducted.

The goals related to the objective of this thesis are:

- Presenting a numerical framework that closely relates the density and level-set methods to each other to have the most fair comparison between the two approaches.

- Compare these two methods to common design cases in literature and additional alternative design cases to highlight key features.

- Solve the design case of the Chest Master and compare the performance to existing solutions.

1.4   Thesis outline

The remainder of this thesis is structured as follows: Section 2 introduces the key aspects of topology optimization for vibration problems. The finite element model, algorithm, objective function and common problems are presented. Section 3 describes the details for the implemented density method. This section also describes the sensitivity analysis, which is also used in the level-set approach. The level-set approach is described in Section 4. Furthermore, Section 5 presents the optimization strategy, comparison criteria and benchmark cases. Where after Section 6 presents the overall results of the design cases with the use of the density and and level-set approach. Section 7 shows the design case of the Chest Master, where two different studies will show the differences with the use of both the density an level-set approach. Finally, Section 8 presents the conclusions and future research topics drawn from this study.

2 Topology optimization

2.1 Structural optimization

Structural and multidisciplinary optimization is the field of optimization that spans a wide variety of methods, which solve a given optimization problem for its structural performance. Such an optimization problem can be classified into different disciplines including: mechanical, fluids, acoustics, biomedical, optics and more [Wang et al., 2021]. They all have the same goal in common, which aims at optimizing the geometric features and the connectivity within a design domain. Three common methods include: shape optimization, size optimization and topology optimization. Shape optimization can be characterized as contour optimization of a structure, without changing the connectivity of its structural members. Size optimization can be characterized as optimizing the dimensions of structural members of a truss or shell structure by e.g. changing the length or cross-sectional area. These two optimization methods are limited to the set of outcomes by their pre-defined assumptions about the design space. This is where topology optimization can alleviate the problems of shape and size optimization. Topology optimization is characterized by having more design freedom, as the geometric features, their size and connectivity within the design domain is being optimized in a unified framework. Additionally, it has the advantage that no initial design parameterization is needed, which in turn can result in more complex final designs.
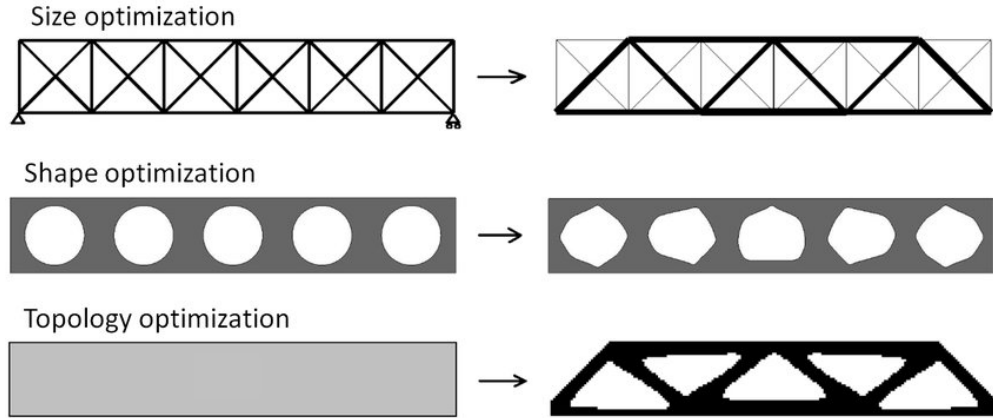

Figure 4: Comparison of different structural optimization techniques from Bendsøe and Sigmund [2004]

In this work, the optimization is focused on optimizing the performance of structures that are subjected to vibrations. The three most frequently used techniques in literature to solve topology optimization problem for vibrations are classified into:

- Evolutionary optimization,

- Density based optimization,

- Level-set based optimization.

In the evolutionary optimization method the material that contributes the least to the rejection criterion is gradually removed. This process is repeated until the values of all elements are within a given range of the rejection criterion. Density-based methods are the most widely used approach for topology optimization. It defines a material density distribution with a value between zero and one. The specific properties that are used in the problem depend on the relevant physics (e.g. elasticity, conductivity, etc.). In level-set based topology optimization, the design geometry is defined by the iso-level of one or several level-set functions. The material interface, that intersects this contour, is defined as the interface between the solid and void regions.
In this work the use of the density based method (Section 3) and the level-set method (Section 4) will be compared to one another, as they are superior in the last few years in the field of topology optimization.

2.2   Finite element model

The finite element model is a key feature in topology optimization process, as the eigenvalues and eigenmodes are calculated from this model. There are two types of elements that are used in this work, namely 2D 4-node quadrilateral plane stress elements with 8 degrees of freedom (DOF) and 2D 4-node quadrilateral Mindlin-Reissner plate elements with 12 DOF [Bathe and Brezzi, 1985] [Hassan et al., 2020]. These element types are non Jacobian-integrated, therefore only simple geometric representations are shown in this work. With either the plane stress or Mindlin-Reissner plate elements the elemental mass and stiffness matrix are constructed. Thereafter, the global stiffness and mass matrix can be constructed, where the eigenvalue computation is calculated from. With the obtained global mass and stiffness matrix the eigenvalues can be computed via Equation 1.

$$\mathbf{K}\phi_j = \lambda_j \mathbf{M}\phi_j, \qquad\qquad j = 1, .., J, \tag{1}$$

$$\phi_j^T \mathbf{M}\phi_k = \delta_{jk}, \qquad j \geq k, \qquad k, j = 1, .., J, \tag{2}$$

Here $\mathbf{K}$ is the global stiffness matrix, $\mathbf{M}$ is the global mass matrix, ϕ_j is the jth eigenvector, ϕ_k is the kth eigenvector, λ_j is the jth eigenvalue, δ_{jk} is the Kronecker's delta and J is the maximal amount of eigenvalues that is taken into account. The dynamic Equation is represented by Equation 1 and it will be assumed that the eigenvectors are orthonormalized via Equation 2. The eigenvalue is related to the eigenfrequency as

$$\omega_j = \sqrt{\lambda_j} \tag{3}$$

Here ω_j is the jth eigenfrequency in radians per second. Finally, the eigenvalue computation is performed in a MATLAB [2021] environment though the sparse solver *eigs*. This in turn results in the eigenvalues and eigenmodes for the specified geometry.

2.3   Algorithms

Most topology optimization problems rely on gradient based algorithms, because solving a large number of function evaluations is an inefficient process. Gradient based algorithms use the function values and their gradients to find the most optimal objective function for large dimensions and numerous constraints [Kim et al., 2021]. Some gradient based algorithms use the information of the Hessian matrix, which can accelerate convergence, but it requires a huge amount of memory and is computationally expensive to calculate. Therefore, most topology optimization problems use Hessian free algorithms such as the optimality criteria (OC) method, method of moving asymptotes (MMA) [Svanberg, 1987] or its globally convergent counterpart (GCMMA) [Svanberg, 2007]. Other methods like convex linearization (CONLIN), interior point optimizer (IPOPT) and sparse nonlinear optimizer (SNOPT) also use gradient based information. However, the OC, MMA and GCMMA algorithms are often superior compared to CONLIN, IPOPT and SNOPT [Sigmund and Maute, 2013]. In topology optimization for vibration problems, there are often multiple constraints present during the optimization process. The OC is a robust algorithm, however it is limited to only one cheap-to-evaluate equality constraint, which limits its functionality in vibration optimization. In this work the use of MMA is used for its flexibility of using multiple constraints and general availability.

2.4   Problem formulations

Problems of topology optimization for vibration problems have various sorts of objective functions. The most frequently used method is maximization of fundamental eigenfrequency. Other methods that have been used in literature and whose will be used in this thesis are: bound formulation for maximizing the nth eigenfrequency, maximizing a distance (gap) between two consecutive eigenfrequencies or synthesizing a specific eigenfrequency. For convenience the eigenvalues are represented in the following problem formulations.

2.4.1 Maximization of fundamental eigenvalues

Maximizing the fundamental eigenvalue is been widely considered in many papers, e.g. ([Ma et al., 1993], [Ma et al., 1995], [Pedersen, 2000]). A frequently used formulation in literature to maximize a set of eigenfrequencies is the sum of reciprocal eigenvalues [Ma et al., 1995]. However, in this work the use of a bound formulation is adopted, as it is able to achieve more improved performance of the objective function [Du and Olhoff, 2007]. In this formulation it is assumed that the damping can be neglected and only a volume constrained is implemented.

$$\max_{\rho_1,..,\rho_N} \left\{ \min_{j=1,..J} \{\lambda_j\} \right\}, \tag{4a}$$

$$s.t.: \quad \mathbf{K}\phi_j = \lambda_j \mathbf{M}\phi_j, \qquad\qquad j = 1,..,J, \tag{4b}$$

$$\phi_j^T \mathbf{M}\phi_k = \delta_{jk}, \qquad j \geq k, \qquad k,j = 1,..,J, \tag{4c}$$

$$\sum_{e=1}^{N_E} \rho_e V_e - V^* \leq 0, \qquad\qquad V^* = \alpha V_0, \tag{4d}$$

$$0 < \rho_{min} \leq \rho_e \leq 1, \qquad\qquad e = 1,2,...,N_e. \tag{4e}$$

In these Equations λ_j is the jth eigenvalue and ϕ_j is the corresponding eigenvector, $\mathbf{K}$ and $\mathbf{M}$ are the symmetric and positive definite stiffness and mass matrix of the whole structure, the value ρ_e is the elemental density value, V_e is the elemental volumetric volume, V_0 is the original volume and α is volume factor of the structure. To avoid singularity in the stiffness matrix, a very small value for the elemental density is taken as ρ_{min}. In this work a value of $\rho_{min} = 10^{-9}$ is taken. The value of N_e represents the total amount of elements in the finite element model. It is assumed that the eigenvectors are mass orthonormalized via Equation 2, where the δ_{jk} is the Kronecker delta. The J value is the maximal amount of eigenvalues to be considered and can be represented as

$$0 < \lambda_1 \leq \lambda_2 \leq ... \leq \lambda_J.$$

2.4.2 Bound formulation for maximization of the nth eigenvalue

A more general approach of maximizing the nth order eigenvalue λ_n is to adopt the bound formulation [Olhoff, 1989]. The bound formulation is more efficient for max-min and min-max optimization problems than the optimization method of Equation 4a. The bound formulation is formulated as

$$\max_{\beta,\rho_1,..,\rho_N} \{\beta\}, \tag{5a}$$

$$s.t.: \quad \beta - \lambda_j \leq 0, \qquad j = n, n+1,..,J, \tag{5b}$$

$$\text{Constraints}: \quad \text{Equations}(1\text{-}4e). \tag{5c}$$

In this formulation the scalar variable β works as variable for the lower bound of the nth eigenvalue to be optimized, as well for mode switching and multiplicity. Additionally, it plays the role as the objective function to be optimized. The variable n in this formulation is the order of the eigenvalue to be optimized i.e. $n = 1$ for the first order or $n > 1$ for higher order eigenvalues. The value for J is assumed to be larger than the highest order of an eigenvalue that can exchange its order with order n that is to be optimized e.g. if the first 2 modes have multiplicity during any point in the optimization than $J \geq 3$ is to be considered.

2.4.3   Bound formulation for maximizing the distance between two consecutive eigenvalues

The bound formulation can also be used to separate two adjacent eigenvalues [Jensen and Pedersen, 2006]. In this process two bound parameters are introduced where one acts to increase the eigenvalues of order $n + 1$, whereas the other bound parameter decreases the eigenvalues below order n. This separation of two eigenvalues can be formulated as

$$\max_{\beta_1, \beta_2, \rho_1, .., \rho_N} \{\beta_2 - \beta_1\}, \tag{6a}$$

$$s.t.: \quad \lambda_j - \beta_1 \leq 0, \qquad j = 1, .., n, \tag{6b}$$

$$\beta_2 - \lambda_j \leq 0, \qquad j = n + 1, .., J, \tag{6c}$$

$$\text{Constraints}: \quad \text{Equations(1-4e)}. \tag{6d}$$

2.4.4   Optimizing for a specific eigenvalue

There are applications where a certain eigenvalue must be synthesized for performance of the vibration application. In this case, the square error of the specific eigenvalue must be minimized to synthesize a specific eigenvalue. Unlike the previous formulation for maximizing the eigenvalues, this is the only minimization problem. The optimization objective function is defined as

$$\min_{\beta, \rho_1, .., \rho_N} \left\{ \frac{(\lambda_k - \lambda_o)^2}{\lambda_o^2} \right\}, \quad k = 1, \tag{7a}$$

$$s.t.: \quad \beta - \lambda_j \leq 0, \qquad j = k + 1, .., J, \tag{7b}$$

$$\text{Constraints}: \quad \text{Equations(1-4e)}. \tag{7c}$$

In this formulation the term λ_o is defined as the objective eigenvalue, k is the first order eigenvalue that will be synthesized to the objective eigenvalue, j is the order of the eigenvalue and J is the maximal order of eigenvalues taken into account where $J \geq 2$. In this thesis only the first eigenvalue will be synthesized for a specific eigenvalue. It is possible to synthesize a higher order eigenvalue for a specific value, however that is not within the scope of this thesis. Furthermore, the square terms are involved to keep the objective function positive definite. Also, in the constraints the β term is still involved as seen with the bound formulation. This term ensures that no higher order modes interfere with the specified eigenvalue.

2.5   Localized eigenmodes

In the context of topology optimization for vibration problems, the main problem that occurs is the presence of localized eigenmodes. Localized modes are a consequence due to the existence of low density areas. These low density areas are very flexible and thus control the lowest eigenmodes of the system. A visual example of a localized eigenmode is shown in Figure 5. In a vibration FE analysis a set of eigenfrequencies are calculated to obtain the desired eigenfrequency range. When low frequency eigenmodes occur, they reduce the range of the original set of eigenfrequencies. In the post processing these can be easily identified, however more eigenmodes have to be calculated to obtain the eigenmodes in the desired frequency range. Calculating more eigenmodes is a computationally expensive process. There are many research papers that eliminate this problem with different techniques. Techniques like removing the elements [Yoon, 2010], [Behrou et al., 2021] or using a density approach that has a non zero gradient for $\rho = 0$ and keeps the ratio of stiffness and mass of low density elements equal [Sigmund and Maute, 2013], [Kang et al., 2020], [Liao et al., 2021]. Although there is a variety of literature that prevents the occurance of localized eigenmodes, there is still a possibility that it occurs in density based topology optimization. Therefore, this thesis will investigate if the level-set formulation can prevent the occurrence of these localized eigenmodes.

Figure 5: Eigenmode representation of a localized eigenmode.

2.6   Multiplicity

Aside from the occurrence of localized eigenmodes in topology optimization for vibration problems, the occurrence of multiplicity adds some extra complications in the optimization process. Multiplicity is the condition where two or more eigenmodes have the same eigenvalue. This condition can occur at the start of the optimization process due to e.g. structural symmetry, or it can happen during the optimization process due to design changes. In general, multiplicity is preferably avoided in structural optimization, as the multiple eigenvalue manifest itself in different eigenmodes. Obtaining sensitivities of a multiple eigenvalue introduces some extra conditions to take into account (explained in Section 3.3.2), which increases the computation time.

3   Density based approach

One of the first methods to solve topology optimization problems was the homogenization technique proposed by Bendsøe [1989]. In the homogenization method the structure is evaluated as a microstructure with holes or squares. The structure elements are then penalized to converge to an optimal solution. There are several variables per element and the microstructure needs to be updated every iteration. This makes the homogenization method complex to implement and computationally expensive [Rozvany, 2009]. A problem that arises is that converging to the optimal microstructure resulted in weak penalization of the elements. Therefore, the final solution results in non-discrete solutions with a grey representation.

3.1   Material interpolation for vibrating structures

One of the most popular methods that is used nowadays in the field of topology optimization is the technique proposed by Bendsøe [1989], which is based on the density of material elements. This new method would later be called the solid isotropic material with penalization method (SIMP) by Rozvany et al. [1992]. It was introduced to reduce the complexity of the homogenization approach and the convergence rate of the 0 (void) - 1 (solid) solutions. In this method the elements of the discretized model are given a density that varies in a continuous way between 0 and 1. By giving the elements this pseudo-density, the algorithm evaluates the effects of adding or removing these elements on the objective function. The SIMP method is expressed as

$$\mathbf{M} = \sum_{e=1}^{N_E} \rho_e^q \mathbf{M}_e^*, \quad \mathbf{K} = \sum_{e=1}^{N_E} \rho_e^p \mathbf{K}_e^*, \quad 0 < \rho_{min} \le \rho_e \le 1. \tag{8}$$

Here ρ_e is the element density value, ρ_{min} is the minimal value of the element density variable, N_e is the total amount of elements in the design domain, $\mathbf{M}_e^*$ is the element mass matrix, $\mathbf{K}_e^*$ is the element stiffness matrix, q is the mass penalty factor and p is the stiffness penalty factor. A common value for q is 1, whereas the value for p is either fixed at a value $p \ge 1$ or increased in a continuation method. The penalization is applied in the intermediate density areas, where the pseudo density gets a value between 0 and 1. These intermediate density areas (grey areas) do not have a physical meaning, only the integer values of 0 and 1 represent a void or solid area. The bigger the penalty factor, the bigger the contrast is between the solid and void areas. The penalty factor that is assigned is an arbitrary number and does not relate to a physical value. A proper choice is dependent on the optimization problem and is non-unique.

A problem that can arise using the SIMP interpolation method, is that the penalized elemental stiffness values can have a very low value compared to the elemental mass value. Therefore, the ratio of the stiffness and the mass is very small. This may lead to the occurrence of localized eigenmodes with a low eigenfrequency. There are various interpolation methods to eliminate the occurrence of localized eigenmodes. The most frequently used methods in literature are: the modified SIMP by Tcherniak [2002] and by Pedersen [2000], the rational approximation of material properties (RAMP) by Stolpe and Svanberg [2001] or the polynomial interpolation by Zhu et al. [2009]. A detailed comparison of various material interpolation methods for vibration applications is done by Huigsloot et al. [2018]. In this work it was found that a linear interpolation method results in the best performing designs. The recommendation is to apply a penalization of intermediate densities elsewhere.

In this work, the modified SIMP method proposed by Tcherniak [2002] is adopted. The method of Tcherniak is based on setting the elemental mass value to 0 in elements with a low material density. This in turn results in a large stiffness to mass ratio, therefore eliminating the spurious localized eigenmodes. The interpolation Equation is described by Equation 9.

$$\mathbf{M}_e(\rho_e) = \begin{cases} \rho_e \mathbf{M}_e^*, & \rho_e > 0.1. \\ \rho_e^r \mathbf{M}_e^*, & \rho_e \le 0.1. \end{cases} \tag{9}$$

The value for r is chosen such that the penalization of the elements below the threshold value of 0.1, will be penalized with a larger factor than the stiffness. As the stiffness penalization is chosen at a factor $p = 3$,

the penalization of the mass is chosen as $r = 6$. The formulation in Equation 9 introduces a discontinuity at the density value of 0.1. To solve this discontinuity, a continuous interpolation function for the mass is to be implemented. This function is represented in Equation 10.

$$\mathbf{M}_e(\rho_e) = \begin{cases} \rho_e \mathbf{M}_e^*, & \rho_e > 0.1. \\ (c_1 \rho_e^6 + c_2 \rho_e^7)\mathbf{M}_e^*, & \rho_e \leq 0.1. \end{cases} \tag{10}$$

Here the two coefficients $c_1 = 6 \times 10^5$ and $c_2 = -5 \times 10^6$ ensures continuity at the value $\rho = 0.1$. Figure 6 shows the ratio of the stiffness over the mass of the SIMP and the modified SIMP technique. As the design variable is reaching 0, the ratio of the becomes very large. This ensures that elements with a low density value are very stiff relative to their mass, essentially preventing the occurrence of localized eigenmodes.
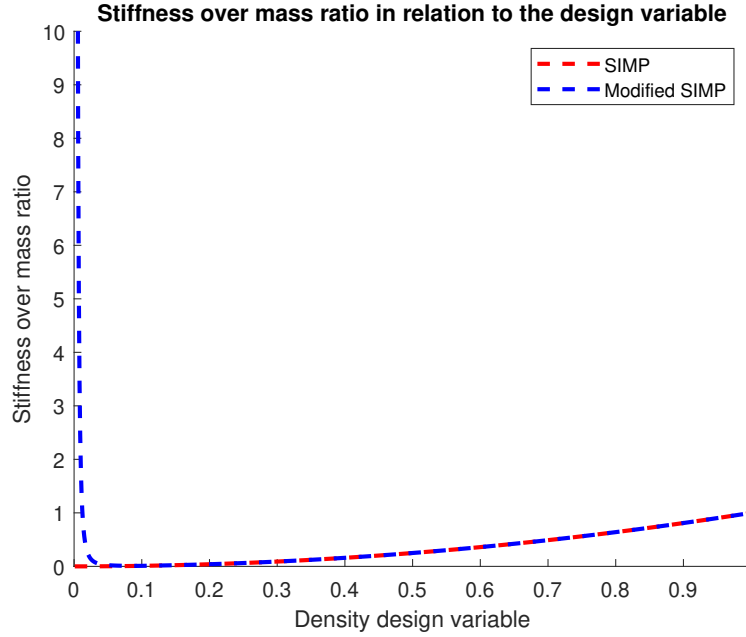
Figure 6: Stiffness over mass ratio of the SIMP interpolation and modified SIMP interpolation function

3.2   Filtering

One of the very first filter schemes was proposed by Sigmund [1994]. The paper describes how the problem of checkerboarding and mesh-dependency can be alleviated via filtering the optimization problem. From this point on, several filtering techniques and schemes have been proposed. They all have different properties and parameters to influence the final outcome of the design. In the "ideal filter method" one could say that the following points are of interest [Sigmund, 2007]:

1. Mesh independence and checkerboard prevention

2. Discrete solutions in (0-1) form by removing grey areas

3. Manufacturability features

4. No extra constraints

5. Limited tuning parameters

6. Stability and fast convergence rate

7. Robustness and general applicability

8. Simplicity and implementation friendly

9. Computation friendly

Depending on the design problem and the user application, e.g. from an academic viewpoint compared to that for industrial use, the list can have a different priority order. In the following sections three common filter types are presented, which will be applied in this thesis.

3.2.1   Density filter

The working principle of density based filters is to modify the element density based on its neighbourhood element densities by some function. The filter has been proposed by Bruns and Tortorelli [2001] and is described by the following Equation

$$\tilde{\rho}_e = \frac{\sum\limits_{i \in N_e} w(\mathbf{x}_i) v_i \rho_i}{\sum\limits_{i \in N_e} w(\mathbf{x}_i) v_i}. \tag{11}$$

The modified element density is denoted by $\tilde{\rho}_e$ and is a function of the neighbour elements by $\rho_{i \in N_e}$. Here N_e is the set of elements within the filter radius R for domain element i, v_i is the elemental volume and $w(\mathbf{x}_i)$ represents a weighting function that is described by a cone function

$$w(\mathbf{x}_i) = R - \parallel \mathbf{x}_i - \mathbf{x}_j \parallel . \tag{12}$$

Here R is the filter radius and $\mathbf{x_i}$ and $\mathbf{x_j}$ represent the the central coordinates of the cell i and j respectively. An important aspect of the density filter is that the volume is preserved in the filter operation. This means that the volume before filtering must stay the same after the filtering. A modified density filter like the Heaviside filter violates this rule. As long as the volume fraction constraint is modified accordingly such that there are no fixed solid and void regions present in the design domain this should not impose a problem [Sigmund, 2007].

3.2.2   Density filtering with a Heaviside step function

A downside of the density filter is that boundaries become blurry. To alleviate this problem a Heaviside step function can be applied to the density filter. A Heaviside density filter [Guest et al., 2004] and a Heaviside step with modified density filter [Sigmund, 2007] have been proposed in early literature. These filters reduce the grey areas produced by the basic density filter. However, a downside of these two Heaviside filters is that they can be prone to poor convergence, as there are volume preservation issues. To alleviate the volume preservation problem, the development of a new filter based on the Heaviside function with volume preservation is proposed by Xu et al. [2010]. Later this filter is simplified by Wang et al. [2011] and represented in the following Equation

$$\bar{\tilde{\rho}}_e = \frac{tanh(\beta\eta) + tanh(\beta(\tilde{\rho}_e - \eta))}{tanh(\beta\eta) + tanh(\beta(1 - \eta))}. \tag{13}$$

In this work the use of the Heaviside function in combination with the density filter will be referred to as the Heaviside filter.

3.2.3   Sensitivity filter

The sensitivity filter was proposed by Sigmund [1997] and describes how the sensitivity of a function can be used as a filter. The filter is represented in Equation 14.

$$\frac{\partial \tilde{f}}{\partial \rho_e} = \frac{\sum\limits_{i \in N_e} w(\mathbf{x}_i) \rho_i \dfrac{\partial f}{\partial \rho_i}}{\rho_e \sum\limits_{i \in N_e} w(\mathbf{x}_i)}. \tag{14}$$

Where f is an objective function specified to the optimization problem and ρ_e in the denominator is a value of $max\{\rho_e, \varepsilon\}$ where ε is a very small number (e.g. ρ_{min}). A key element of the elemental sensitivities is that the design updates are based on filtered sensitivities, instead of real sensitivities. The filter blurs the sensitivities over the neighbouring elements, due to the filter operator. nonetheless it has been very popular in literature and is still used in recent literature, e.g. Zhou et al. [2017], Kang et al. [2020], Xia et al. [2021].

3.3 Sensitivity analysis

The sensitivities of eigenvalues can be divided into two parts: uni-modal (simple) eigenvalues and multi-modal (multiple) eigenvalues. Simple eigenvalues impose no problem for the sensitivity calculation, as the eigenmode is distinctive and differentiable. On the other hand, a multiple eigenvalue cannot be calculated straightforward, because of the lack of usual differentiability properties of the subspace spanned by the eigenvectors associated with the multiple eigenvalue [Du and Olhoff, 2007]. In this work, the sensitivity analysis used in Seyranian et al. [1994], Jensen and Pedersen [2006] and Du and Olhoff [2007] will be followed. The sensitivity analysis can distinguish sensitivities of simple and multiple eigenvalues.

3.3.1 Simple eigenvalues

Simple eigenvalues are relatively easy to solve, as the eigenvectors are unique. A simple jth eigenvalue is defined as i.e. $\lambda_{j-1} < \lambda_j < \lambda_{j+1}$ and has a corresponding eigenvector ϕ_j, which is unique. To determine the sensitivity of the eigenvalues, Equation 1 is differentiated with respect to the design variable ρ_e resulting in

$$\left(\frac{\partial \mathbf{K}}{\partial \rho_e} - \lambda_j \frac{\partial \mathbf{M}}{\partial \rho_e} - \frac{\partial \lambda_j}{\partial \rho_e} \mathbf{M} \right) \phi_j + \left(\mathbf{K} - \lambda_j \mathbf{M} \right) \frac{\partial \phi_j}{\partial \rho_e} = 0, \qquad e = 1, .., N_e. \tag{15}$$

Equation 15 can be further simplified by premultiplying by ϕ_j^T and make use of the normalization in Equation 2 and the vibration Equation 1 [Wittrick, 1962], [Courant and Hilbert, 2007]. This results in

$$\frac{\partial \lambda_j}{\partial \rho_e} = \phi_j^T \left(\frac{\partial \mathbf{K}}{\partial \rho_e} - \lambda_j \frac{\partial \mathbf{M}}{\partial \rho_e} \right) \phi_j, \qquad e = 1, .., N_e. \tag{16}$$

The derivatives of the global mass and stiffness matrix can be obtained via the material model (see Equation 8) resulting in

$$\frac{\partial \mathbf{K}}{\partial \rho_e} = p \rho_e^{(p-1)} \mathbf{K}_e^*, \qquad \frac{\partial \mathbf{M}}{\partial \rho_e} = q \rho_e^{(q-1)} \mathbf{M}_e^*, \qquad e = 1, .., N_e. \tag{17}$$

Combining Equation 17 and Equation 16 the resulting derivative for the vibration Equation becomes

$$\frac{\partial \lambda_j}{\partial \rho_e} = \phi_j^T \left(p \rho_e^{(p-1)} \mathbf{K}_e^* - \lambda_j q \rho_e^{(q-1)} \mathbf{M}_e^* \right) \phi_j, \quad e = 1, .., N_e. \tag{18}$$

The sensitivities of simple eigenvalues in Equation 18 can be used as an input to solve a given vibration problem via e.g. a mathematical programming algorithm such as MMA.

3.3.2 Multimodal eigenvalues

Multiple eigenvalues manifest themselves in different ways during an optimization process. They can be multiple from the beginning of the optimization due to structural symmetry, or they can coalesce during the optimization process. In multiplicity conditions there is no unique eigenvector. This means that any linear combination of the eigenvectors will satisfy the original eigenvalue problem [Seyranian et al., 1994] i.e. this eigenvector of linear combination is also an eigenvector of the eigenvalue at multiplicity [Jensen and Pedersen, 2006]. To determine whether eigenvalues are multimodal, a relative difference between the eigenmodes is determined as

$$r = \frac{|\lambda_{i+j} - \lambda_i|}{\lambda_i}, \qquad i = 1, .., J - 1, \qquad j = 1, ..J - i. \tag{19}$$

If the value for r is lower than a certain threshold value, which in this work is taken as $r \leq 0.05$, then the corresponding eigenvalues have multiplicity. The value J is the amount of eigenvalues in the optimization process. When a solution of the generalized eigenvalue problem results in an M fold multiple eigenvalue

$$\tilde{\lambda} = \lambda_i, \qquad i = m, .., m + M - 1. \tag{20}$$

Here $\tilde{\lambda}$ is the set of M fold multiple eigenvalue. The m is the first eigenvalue that has multiplicity and M is the amount of eigenvalues in multiplicity e.g. if the third and fourth eigenvalue have multiplicity, then $m = 3$ and $M = 2$. To determine the sensitivities corresponding to the multiple eigenvalue, a set of eigenvectors need to be found that satisfies the following conditions

$$\sum_{i=m}^{i} a_i \phi_i = \overline{\phi}, \qquad i = m, .., m + M - 1, \tag{21}$$

$$\sum_{i=m}^{i} a_i^2 = 1, \quad \Rightarrow \quad \overline{\phi}^T \mathbf{M} \overline{\phi} = 1. \tag{22}$$

Here ϕ_i are the eigenvectors corresponding to the multiple eigenvalue, the coefficients a_i are to be determined. By inserting Equation 21 into Equation 16 and taking the extreme values for $\dfrac{\partial \lambda_j}{\partial \rho_e}$ with respect to the constants a_i and setting this equal to zero the following expression is obtained

$$\underbrace{\begin{pmatrix} g_{1,1} & g_{1,2} & \cdots & g_{1,k} \\ g_{2,1} & g_{2,2} & \cdots & g_{2,k} \\ \vdots & \vdots & \ddots & \vdots \\ g_{s,1} & g_{s,2} & \cdots & g_{s,k} \end{pmatrix}}_{\text{G matrix}} \begin{Bmatrix} a_1 \\ a_2 \\ \vdots \\ a_i \end{Bmatrix} = \begin{Bmatrix} 0 \\ 0 \\ \vdots \\ 0 \end{Bmatrix}, \tag{23}$$

$$g_{sk} = \phi_s^T \left(\frac{\partial \mathbf{K}}{\partial \rho_e} - \lambda_j \frac{\partial \mathbf{M}}{\partial \rho_e} \right) \phi_k, \qquad s, k = m, .., m + M - 1 \tag{24}$$

The values for s and k correspond to the eigenvectors in the multiple eigenvalue calculated in Equation 1 and the value for λ_j is chosen as the lowest value of λ of the multiple eigenvalues. The eigenvalue of the G matrix defines the direction of each eigenvector corresponding to the multiple eigenvalue. Consequently, this eigenvalue corresponds to the sensitivity of the multiple eigenmode.

$$\det\left([G - \Lambda I]\right) \tag{25}$$

$$\frac{\partial \lambda_j}{\partial \rho_e} = \Lambda_i, \qquad i = m, .., m + M - 1. \tag{26}$$

In Figure 7 a flowchart for the computational procedure is represented. The first loop where the convergence check is $\dfrac{||\Delta\lambda||}{\lambda} < \zeta$ has a lower error value than in the larger loop, where additionally the convergence of the continuation is checked. The reasoning behind $\zeta > \varepsilon$ is that the final solution should have the highest accuracy, whereas the intermediate updating steps can have a lower accuracy to speed up the simulation time.
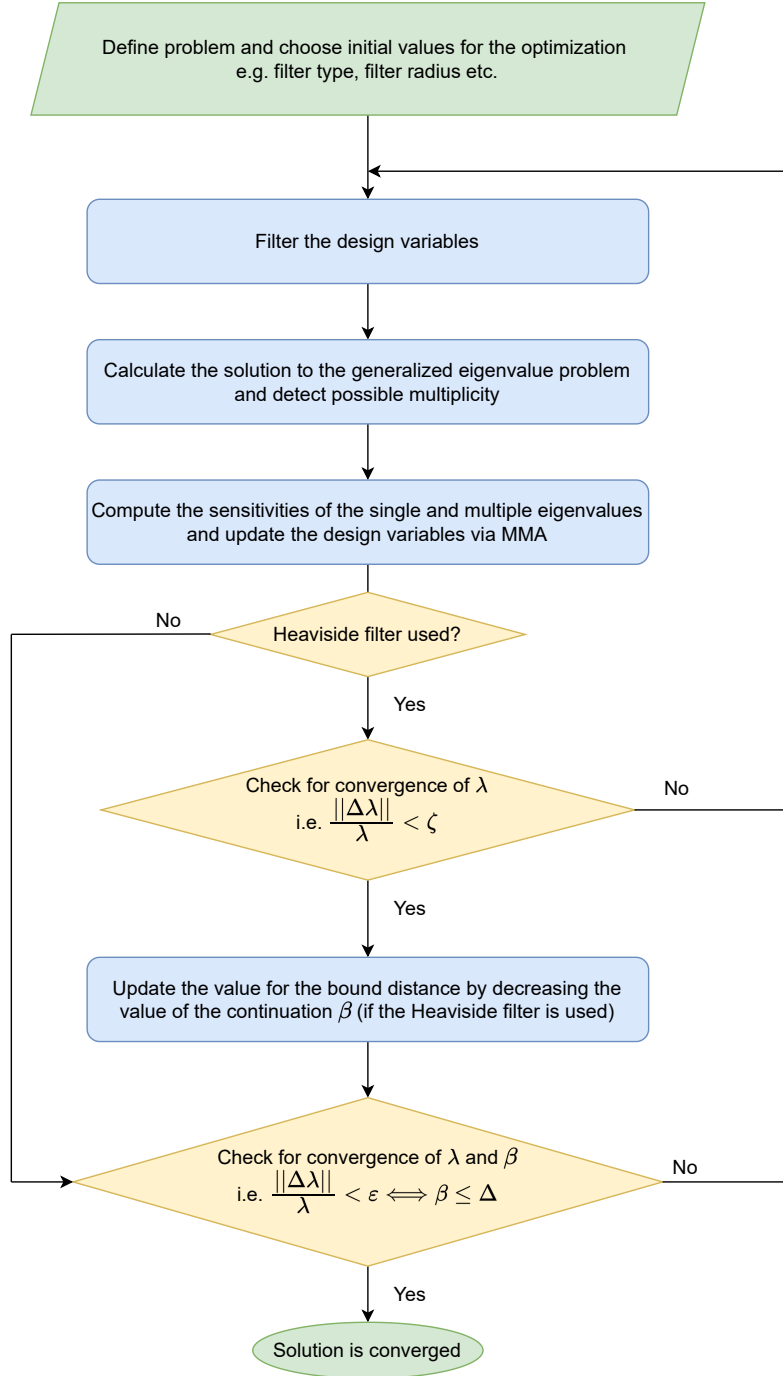
Figure 7: Flowchart of the density method with the update procedure.

4   Level-set based approach

The level-set method (LSM) was first introduced by Osher and Sethian [1988] and works by tracking the motion of moving fronts. Later it was exploited for topology optimization as it allowed moving front without remeshing. This front is represented as an iso-level function c. It is common that the iso-level-set function (LSF) has a value of $c = 0$. In 2D this boundary can be represented as a plane that intersects the LSF. An advantage of using level-set for topology optimization problems is that it allows for a crisp description of interfaces and boundaries [Allaire and Jouve, 2005], [van Dijk et al., 2013], [Sigmund and Maute, 2013], [Zargham et al., 2016]. Furthermore, it is robust to solve different kinds of problems and associated constraints. The geometry of a structure is represented by an iso-level of the level-set function as

$$
\begin{aligned}
\phi(\mathbf{x}) > 0: & \qquad \forall \mathbf{x} \in \Omega & \text{(material domain)}, \\
\phi(\mathbf{x}) = 0: & \qquad \forall \mathbf{x} \in \Gamma & \text{(interface)}, \\
\phi(\mathbf{x}) < 0: & \qquad \forall \mathbf{x} \in D/\Omega & \text{(void domain)}.
\end{aligned}
\tag{27}
$$

The LSM consists out of three general parts, namely the mechanical model, the parameterization and the optimization procedure. The mechanical model includes the discretized structural model and the geometry mapping of level-set function. The geometry mapping projects the parameterized model onto the discretized model, where both the structural model and the geometry mapping influence the performance of the optimization. The material mapping can consist out of 3 types, namely: conforming discretization, immersed boundary with e.g. X-FEM or a volume-fraction-based material mapping called the Ersatz material model. The three different approaches are shown in Figure 8, where the density-based representation is a representation of the Ersatz material model.

(a) Conforming: Only the material domain is discretized.

(b) Immersed Boundary Technique: Boundary conditions are enforced locally at the interface.

(c) Density-based: In each finite element an element density indicates the amount of material.
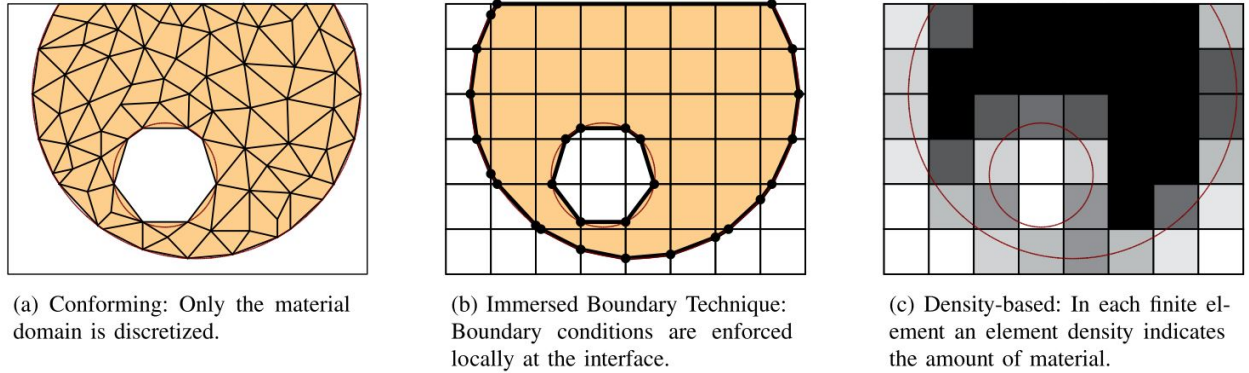
Figure 8: Representation of different geometry mappings for the level-set function, from van Dijk et al. [2013]. The density-based mapping can also be referred to as the Ersatz material model.

The parameterization of the level-set function is controlled by the optimization variables and can be formulated as e.g. FEM shape functions or radial basis functions (RBF). These have various support sizes, which in turn influence the convergence rate, design detail and memory allocation. There are various solvers (e.g. Hamilton-Jacobi methods or a mathematical update procedure) that can solve a level-set based topology optimization problem. These solvers are dependent on sensitivities of the objective function and the constraints of the optimization. The sensitivities can be defined as e.g. Variational shape sensitivities, parameter shape sensitivities, material parameter sensitivities, topological sensitivities or non-sensitivity information [?].

4.1   Level-set parameterization

A popular approach to represent the LSF is via the use of RBF. RBF are radially symmetric functions around defined positions in the mesh to approximate the multivariate scattered data. There are several options to choose from for the representation of the level-set function. Many popular types of parameterization are available in literature, such as thin-plate splines, Gaussians, Compactly Supported Radial Basis Functions

(CSRBF), Multi-Quadratic (MQ) Splines and Inverse Multi-Quadratic (IMQ) Splines [Wei et al., 2018]. These functions vary from local to global interpolation functions with different properties, as seen in Table 1. Local basis functions are often interpreted as FEM shape functions with minimal element overlap. Global basis functions overlap the whole domain and give a non-zero function matrix. A result of this type of interpolation is that all optimization variables have an influence on the change of the design domain. This in turn results in a fast rate of change of the design variables, with the cost of design detail, memory allocation and computation time. On top of that, the incremental step size for updating the design variables is chosen rather arbitrarily, making it design specific to choose this parameter. Another type of basis functions are mid-range basis functions. These basis functions are non-zero over a finite part of the design domain, however they overlap each other by a defined amount of elements. The mid-range type of basis functions ensure a faster rate of convergence compared to local basis functions, as more information of elements is taken into account. Furthermore, these basis functions increase computation efficiency, as they are sparse and strictly positive definite [van Dijk et al., 2013], [Luo et al., 2007]. An example of the overlapping of basis functions is represented in Figure 9 and their corresponding properties Table 1. In this work the use of CSRBF are employed for their numerical efficiency and tunability for design detail.

(a) Local basis functions.   (b) Mid-range basis functions.   (c) Global basis functions.
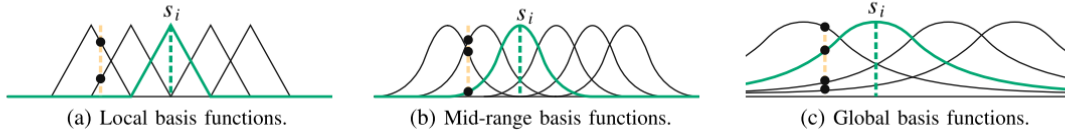
Figure 9: Representation of different sizes of basis functions. The black dots indicate how many basis functions are non-zero at an arbirary location [van Dijk et al., 2013].

In some examples in this work, the level-set function is initially constructed as a function of geometric shapes. These geometric shapes represent holes in the design domain by being cut through the zero level-set plane. These geometric shapes represent the initial configuration of the design and can be altered by changing the position of the circular holes and their radius.

Size of basis function	Design detail	Convergence rate	Memory allocation
Local basis functions	High	Slow	Low
Mid-range basis functions	Medium/High	Medium/High	Low
Global basis functions	Low	High	Very high

Table 1: Basis functions properties

4.1.1   Parameterization using CSRBF

In this work the CSRBF with $2k$ continuity from Wendland [1995], such as the C2, C4 and C6 functions are implemented. The support radius for each CSRBF must be chosen accordingly and is specific for each CSRBF. A trade-off must be made between computational efficiency and ensuring non-singularity. Consequently, when a support radius is too small it will be ineffective to span the inner-constraint gaps with the use of CSRBF, and when a support radius is too large it would increase the computation time [Luo et al., 2007]. Experimental values have to be selected to calculate the most optimal value for the support radius [Buhmann, 2000]. The CSRBF Wendland functions are defined by a radius of support in 2D Euclidean space by

$$r = \frac{\sqrt{(x - x_i)^2 + (y - y_i)^2}}{d_{ml}}. \tag{28}$$

(a) C2 CSRBF representation.   (b) C4 CSRBF representation.   (c) C6 CSRBF representation.
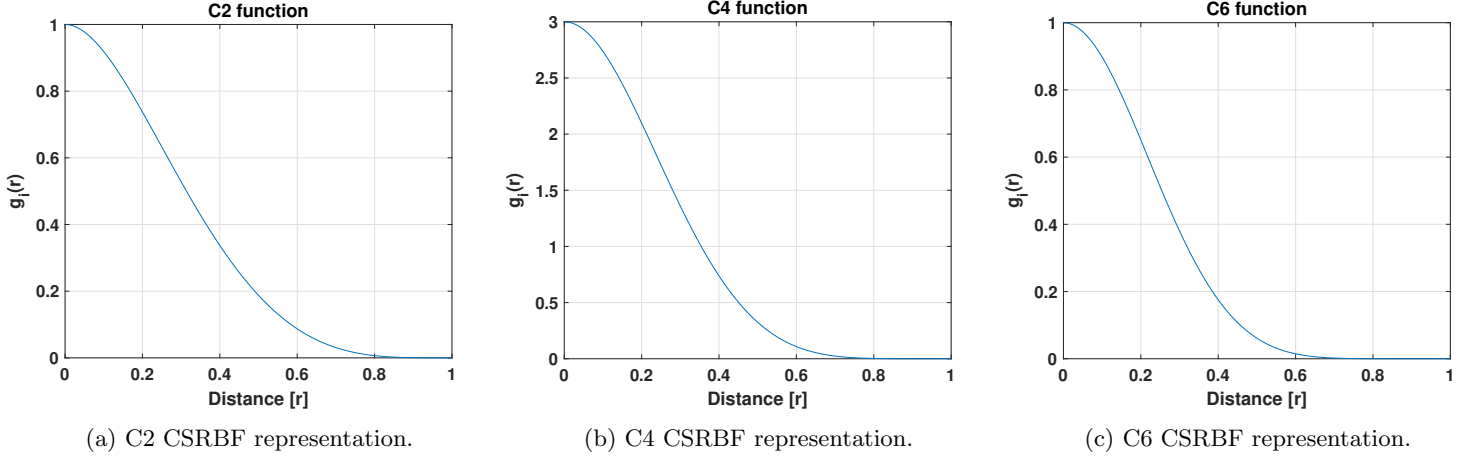
Figure 10: 1D CSRBF representation of Equation 29.

Here (x, y) is the current sample knot of the RBF, (x_i, y_i) are the other knots in the design space and d_{ml} is a scalar parameter that defines the amount of nearby elements that are supported in the radius. The larger the value, the more knots are taken into the calculation of the RBF. The shapes of the CSRBF are defined by Equation 29 and represented by Figure 10.

$$C2 : g_i(r) = \max\{0, (1-r)\}^4 \ (4r + 1), \tag{29a}$$

$$C4 : g_i(r) = \max\{0, (1-r)\}^6 \ (35r^2 + 18r + 3), \tag{29b}$$

$$C6 : g_i(r) = \max\{0, (1-r)\}^8 \ (32r^3 + 25r^2 + 8r + 1). \tag{29c}$$

In general, the low-order CSRBF should have a larger support radius, whereas the higher order CSRBF should have a smaller support radius. The higher order CSRBF might be more sensitive to a variation of the support radius, whereas the lower order CSRBF is more robust to the element radius [Luo et al., 2007]. With the radial basis functions obtained, the level-set function can be described by positioning the basis functions at specified nodes in the design domain. Depending on the geometry mapping (see Section 4.2) a convenient position of the knots is chosen. In this work the density representation is used for the geometry representation. Therefore, the level-set function is solved by the algorithm on the nodes of the mesh elements, where after these nodal values are transformed to the center of the elements to obtain the element density. This can be easily transformed via the $\mathbf{G}$ matrix as seen in Equation 31. The level-set function is then defined by

$$\phi(\mathbf{x}) = \mathbf{G}(\mathbf{x})^T \boldsymbol{\alpha} = \sum_{i=1}^{n} g_i(\mathbf{x})\alpha_i, \qquad n = 1, .., N_n. \tag{30}$$

Where the vector of RBF is defined as

$$\mathbf{G}(\mathbf{x}) = \underbrace{[g_1(\mathbf{x}), g_2(\mathbf{x}), ..., g_n(\mathbf{x})]^T}_{M \times N}, \qquad n = 1, .., N_n. \tag{31}$$

And the vector of the expansion coefficient as

$$\boldsymbol{\alpha} = [\alpha_1, \alpha_2, ..., \alpha_n]^T, \qquad n = 1, .., N_n. \tag{32}$$

Here α is the expansion coefficient of the CSRBF positioned at the knot i, N_n is the number of fixed predefined knots (mesh nodes in this work) and M is the amount of center nodes of the mesh elements. The G matrix acts as an transformation matrix between the mesh nodes and the mesh center elements.

The variables in $\boldsymbol{\alpha}$ are the new optimization variables. Since all knots will be fixed in the same design space, the initial value for $\boldsymbol{\alpha}$ can be determined by inverting the $\mathbf{G}$ matrix and multiplying it by the initial level-set function. This is shown in Equation 33. This initial value of $\boldsymbol{\alpha}$ is to be optimized by any updating procedure.

$$\boldsymbol{\alpha} = \mathbf{G}^{-1}\phi. \tag{33}$$

After the update procedure, that updates the new values of $\boldsymbol{\alpha}$, the level-set function is reconstructed via substituting its value into Equation 30.

4.2   Ersatz material model

As this work is focused on the comparison between the density and the level-set method, a mapping type that has the most similarities with the density method is preferred. In a conventional level-set mapping the geometry mapping is a pure discrete representation of the material model, where Equation 28 defines if the material is solid or void. To map the level-set geometry to a mechanical model using a density distribution, the so called Ersatz material model is implemented [Wang et al., 2003], [Allaire et al., 2004]. The Ersatz material model introduces intermediate densities ρ to represent the material phase by scaling their properties (e.g. Young's modulus), as with the density method. Therefore, the mapping of this material model has similarities with the density based optimization method. In this work the density distribution $0 < \eta \leq \rho(\phi) \leq 1$ is used, where $\rho(\phi)$ is defined as

$$\rho(\phi) = H(\phi). \tag{34}$$

Where $H(\phi)$ is the Heaviside function. In most topology optimization literature with the use of a level-set function they incorporate the exact Heaviside function in Equation 35.

$$H(\phi) = \begin{cases} 0 \text{ for } \phi < 0, \\ 1 \text{ for } \phi \geq 1. \end{cases} \tag{35}$$

The exact Heaviside function produces a crisp black and white description of the design domain, however it is non-differentiable. This can be inconvenient depending on the update procedure for the level-set function. As the Ersatz model is adopted, a continuous representation of the Heaviside function prevents singularity of the non-differentiability of the exact Heaviside function. The function is therefore often replaced by a smooth approximation of the Heaviside function $\tilde{H}(\phi)$ that can be differentiated. The polynomial used in this work is approximated by Equation 36.

$$\tilde{H}(\phi) = \begin{cases} 0 & \text{for } \phi < -h, \\ \dfrac{1}{2} - \dfrac{1}{4}(\dfrac{\phi}{h})^3 + \dfrac{3}{4}(\dfrac{\phi}{h}) & \text{for } -h \leq \phi \leq h, \\ 1 & \text{for } \phi > h. \end{cases} \tag{36}$$

In this equation, h is defined as the bandwidth of the level-set function. It is defined as half the distance between a user-defined upper and lower bound $h = \phi_b/2$

$$\phi_b = \phi_u - \phi_l. \tag{37}$$

The value for the upper bound ϕ_u and the lower bound ϕ_l is not the definition of the maximal and minimal value of the level-set function, rather it indicates a range wherein the density of the elements should be interpolated. This bound is the interface between the solid and void region of the domain. A representation of this bound is shown in Figure 11.
To obtain a more discrete design, the bound parameter should be reduced during the optimization process. Figure 11a starts of with a large bound value, which results in a lot of intermediate density areas (as shown in the lower part of Figure 11a). All of the level-set function values are now considered during the optimization process. Each element is thus a projection of a related level-set function value. This has a similar principle as density based optimization, where the design variable is ρ and has a upper bound of 1 and a lower bound of
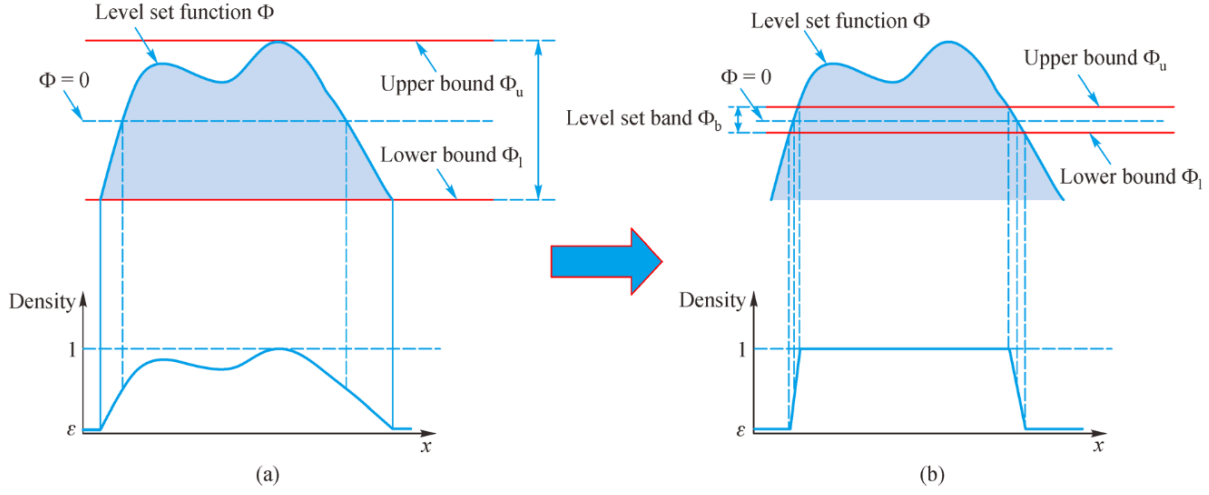
Figure 11: Density interpolation scheme of the level-set band method by gradually reducing ϕ_b [Wei et al., 2020]. (a) Case with a large level-set band between the upper and lower bounds in the beginning stage of the optimization; (b) Case with a small level-set band after convergence.

ε. Unlike the density method, the band ϕ_b of the Heaviside function is reduced to a smaller value during the optimization process, as shown in Figure 11b. When the band distance ϕ_b is considerably small e.g. as small as one element in length, it ensures a more crisp description of the design domain with less intermediate densities [Wei et al., 2020]. This technique has some similarities as with the filters of the density approach. The projection filter, where the β parameter is increased to obtain a more discrete design, works in the same sense. Start off with a large undefined design domain and slowly increase the discreteness to converge to a final design.

There are two expected advantages of topology optimization with the use the level-set function and Ersatz approach compared to conventional level-set approaches. Firstly, conventional level-set formulations update the design by updating the boundary of the zero level contour. Consequently, the initial configuration of the design domain is all-important for the final outcome after the optimization. As the presented technique uses sensitivities of the whole design domain, the initial configuration is less dependent on the final outcome. Additionally, new holes can be nucleated at desired locations without the use of additional techniques as e.g. regularization or velocity extensions. Secondly, the objective function calculations are performed with the interpolated density of the level-set function. This design has a lot of intermediate densities, but almost never disconnected elements. During conventional level-set methods that interpolate over the zero level-set plane, disconnected elements or cracks in the structure can occur as shown in Figure 12 and in Li et al. [2017]. These isolated islands and cracks can produce localized eigenmodes. By using the density representation as geometry for the optimization this phenomena is more prevented, as the density representation is less sensitive to the initial input.

An example of the representation used in this work is shown in Figure 12. There is a level-set representation, which is fully discrete, a density representation used for the optimization and a level-set function of the CSRBF is represented with the boundary layers ϕ_u, ϕ_l and the zero level plane in the middle. If the function is above the zero level plane, the geometry is represented as fully solid material in the level-set representation and below this plane is represented as void. For a fully solid material in the density representation the CSRBF must be above the plane ϕ_u. Consequently, if the CSRBF is below ϕ_l the density representation is void.

Figure 12 clearly shows the expected advantage of the Ersatz model, as the density representation shows 4 connections to the side of the square, while the level-set representation shows an almost disconnected island in the middle of the geometry. A FEM analysis of the zero level-set model would result in either localized eigenmodes or rigid body modes.
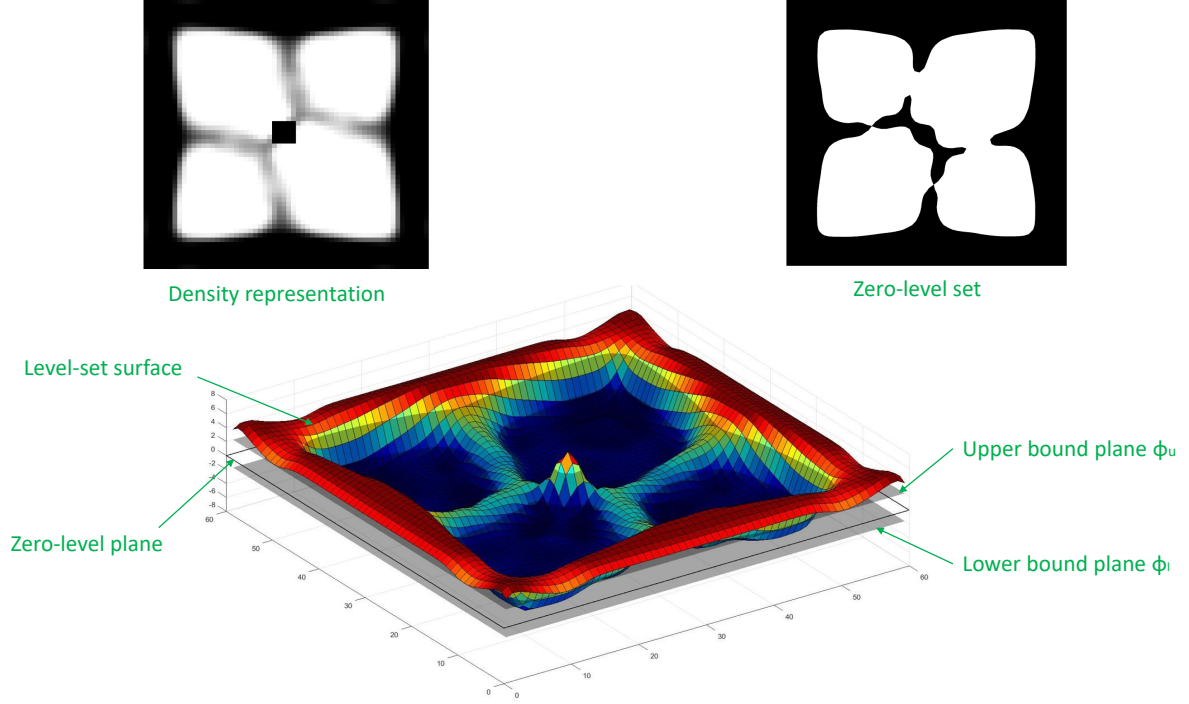
Figure 12: Representation for the level-set optimization, where a density, level-set and zero level-set representation is shown. The band of the upper bound and lower bound have a distance of $\phi_b = 4$.

4.3   Computational procedure

The sensitivity calculation for the level-set method with the use of the Ersatz material model, which is updated via MMA, is not too different from density based optimization approach used in this work. The sensitivities with respect to the eigenvalues are the same as described in Section 3.3. The sensitivities of the Heaviside function and the transformation of the CSRBF are described by

$$\frac{\partial \rho}{\partial \phi} = \frac{\partial \tilde{H}}{\partial \phi} = \begin{cases} 0 & \text{for } \phi < -h, \\ \frac{3}{4}\left(\frac{1}{h} - \frac{\phi^2}{h^3}\right) & \text{for } -h \leq \phi \leq h, \\ 0 & \text{for } \phi > h, \end{cases} \tag{38}$$

$$\frac{\partial \phi}{\partial \boldsymbol{\alpha}} = \mathbf{G}(\mathbf{x})^T. \tag{39}$$

The sensitivities with respect to the original design variables $\boldsymbol{\alpha}$ is obtained by using the chain rule as

$$\frac{\partial f}{\partial \boldsymbol{\alpha}} = \frac{\partial f}{\partial \boldsymbol{\rho}} \frac{\partial \boldsymbol{\rho}}{\partial \boldsymbol{\phi}} \frac{\partial \boldsymbol{\phi}}{\partial \boldsymbol{\alpha}}. \tag{40}$$

Here $\dfrac{\partial f}{\partial \boldsymbol{\rho}}$ for simple eigenvalues is equal to Equation 18 and for a multiple eigenvalue it is equal to Equation 26. Consequently for the volume constraint, the sensitivity calculation is represented as

$$\frac{\partial v}{\partial \boldsymbol{\alpha}} = \frac{\partial v}{\partial \boldsymbol{\rho}} \frac{\partial \boldsymbol{\rho}}{\partial \boldsymbol{\phi}} \frac{\partial \boldsymbol{\phi}}{\partial \boldsymbol{\alpha}}. \tag{41}$$

Here $\dfrac{\partial v}{\partial \boldsymbol{\rho}}$ is the volume derivative of an element, which is equal to 1. Now that we have all the ingredients to solve the eigenvalue problem for the level-set formulation with the Ersatz material model, we can implement this in the program. In Figure 13 a flowchart for the computational procedure is represented. The first loop where the convergence check is $\dfrac{||\Delta\lambda||}{\lambda} < \zeta$ has a lower error value than in the larger loop, where additionally the convergence of the bound is checked. The reasoning behind $\zeta > \varepsilon$ is that the final solution should have the highest accuracy, whereas the intermediate updating steps can have a lower accuracy to speed up the simulation time.
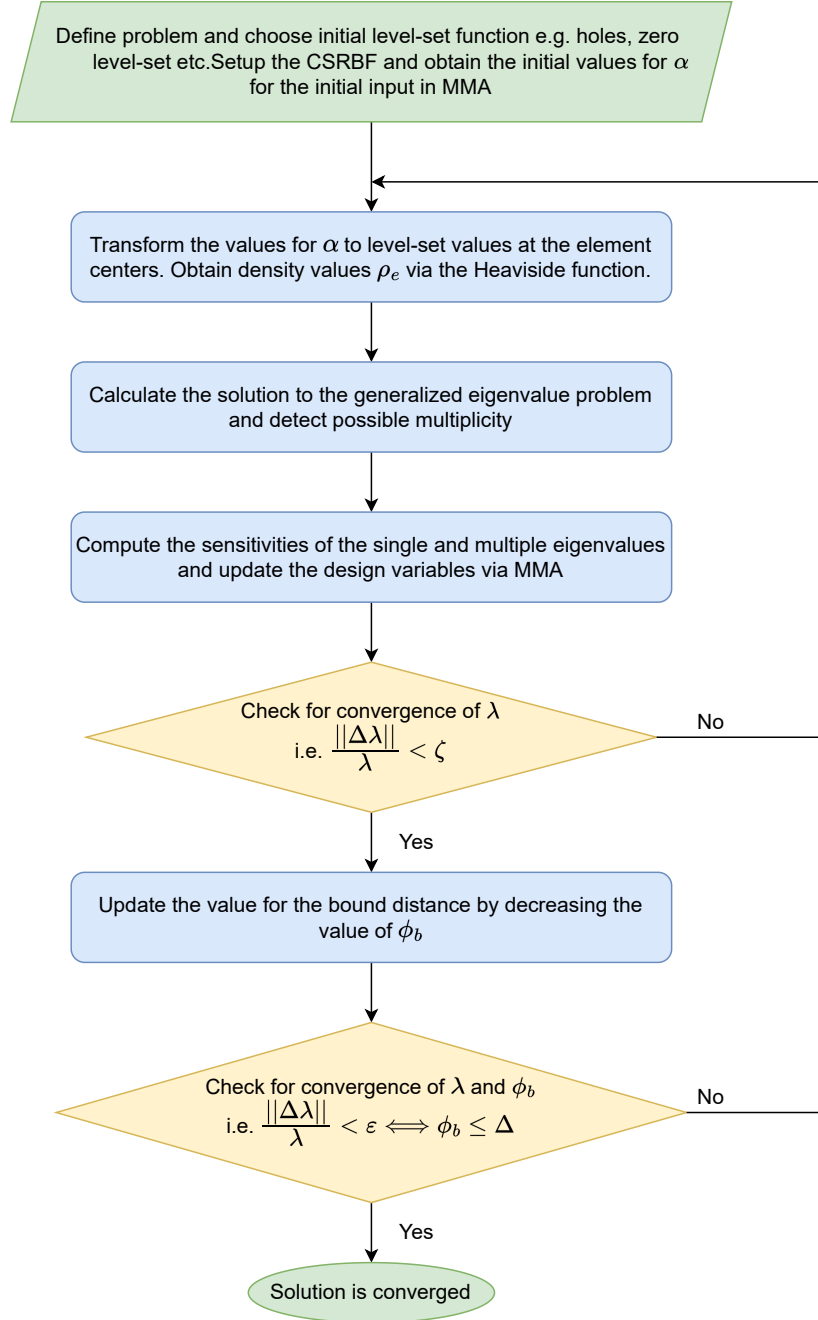
Figure 13: Flowchart of the Ersatz level-set method with a mathematical update procedure.

5   Comparison setup

It is difficult to make a fair comparison between the density and level-set approach, as both methods have different variables that can influence the optimization process. For sure, every design case can be optimized to the fullest for every parameter, however that is not the scope of this thesis. The main goal of the thesis is to display the differences of the presented approaches for their efficiency, stability and practicality in an academic and industrial environment. To be able to tell if one optimization approach performs better, comparable or worse than another, different benchmark cases from literature are used. These benchmark cases have been used throughout literature in e.g. Du and Olhoff [2007], Zhou et al. [2017], Li et al. [2021b] or Liao et al. [2021]. Furthermore, to minimize the influence of the variables and settings of the two methods, a meticulous comparison strategy is presented. This strategy aims to obtain the most fair and optimal comparison as possible between the two methods and their corresponding benchmark cases. Based on this strategy, the most suitable optimization method will be used to solve the Chest Master design case accordingly.

5.1   Comparison strategy

When it comes down to comparing the level-set and density method, numerous setups can be implemented to showcase the differences between them. However, this would result in a long list of solutions, which is impractical from a comparison standpoint. Therefore, a more systematic approach is proposed to highlight the differences between these two approaches. The selection of objective functions, design cases and parameterization have been selected such that it spans a broad range of optimization scenario's. This in turn reduces the amount of results and gives a more concise overview of the differences between the applied techniques. Furthermore, it is desired that the proposed strategy is applicable for future developed techniques to have a similar comparison with the presented techniques. The proposed approach to setup the density and level-set cases for the comparison can be formulated as:

- Firstly, in terms of design cases, there are two types of design problems considered: a 2D beam shape and a 3D symmetric plate, see Figure 14. These benchmark examples have been frequently used in literature, e.g. Du and Olhoff [2007], Yoon [2010], Zhou et al. [2017]. Hence it gives relevant comparative results to existing and possibly newly produced optimisation techniques. There are a variety of boundary conditions proposed to consider a larger set of results.

- Secondly, in terms of objective functions, the maximization of the fundamental eigenvalue is most frequently used in literature. Therefore, this objective function will be used for the beam as well as for the plate design example. Additionally, three objective functions will be included, namely maximization of the second eigenfrequency, maximization of a bandgap and optimizing for a specific eigenfrequency. The goal of using these objective functions is to highlight the differences between the density and level-set approaches, if there are any.

- Thirdly, in terms of parameterization and regularization, to be able to do a concise comparison between the density and level-set method, the amount of adjustable parameters, settings and initial designs should be kept the same. However, as these techniques have method-specific parameters (e.g. design variables), it is difficult to have identical parameter settings for both methods. To ensure a qualitative comparison, it is opted that all methods should converge with minimal changes of the parameters. The only parameters that can be adjusted are the algorithm settings and the continuation settings. However, they are fixed as much as possible to the initially proposed settings in Section 5.4. Only at the occurrence of convergence instabilities the parameters are slightly altered to be able to converge for the given design case.

5.2   Comparison criteria

To compare the level-set and density methods, several criteria are formulated to show the differences of the applied methods. These criteria can be categorized as qualitative or quantitative criteria.
Quantitative criteria are measurable and can be obtained from simulation data. The quantitative criteria from Table 2a used in this work are implemented as follows:

Table 2: Qualitative and quantitative criteria for the comparison.

(a) Quantitative criteria

	M_{nd}	Objective value	Iterations
Unit	%	ω	-

(b) Qualitative criteria.

	Efficiency of applied method	Problems encountered
Keywords	Practicality, fine tuning, sensitivity of parameters	Convergence instability, grey areas, localized eigenmodes

- To measure the discreteness of the final design representation the so-called measure of non-discreteness (M_{nd}) is used as defined in Equation 42. The formulation was first proposed by Sigmund [2007] and is widely used in literature nowadays. In here n stands for the total amount of elements and $\tilde{\rho}_e$ are the element densities. This evaluation of the design domain outputs a result between 0% and a 100%, which indicates how much grey elements are still present. A value of 100% means that the design is fully grey and a value of 0% means that the design is fully discrete.

$$M_{nd} = \frac{\sum_{e=1}^{n} 4\tilde{\rho}_e(1 - \tilde{\rho}_e)}{n} \times 100\%. \tag{42}$$

- The final value of the objective function shows if there is a significant difference in the final result of a selected method. However, one should interpret these results with respect to designs where the final design is not discrete (i.e. a $M_{nd} \geq 10\%$) carefully. If a design is not fully discrete the FEM analysis is not accurate, as the grey areas are undefined material in the design domain.

- There are two convergence criteria proposed that will result in a discrete design and a stable objective function. These criteria are the M_{nd} and the relative difference in objective function, which both have to be satisfied to converge.

$$\sigma = \frac{|\Delta\lambda|}{\lambda} = \frac{|\lambda_{i+1} - \lambda_i|}{\lambda_i}. \tag{43}$$

Here i is the iteration number of the optimization run. In general, it was chosen that the relative difference of the objective function should be $\sigma \leq 0.01\%$ and the final design may not contain more than 5% grey areas. The M_{nd} convergence criterion puts less emphasis on the importance of this value for the quantitative criteria. However, it was opted as it results in a more discrete final design representations. Moreover, it prevents early convergence due to the σ criterion, which could happen early on in the optimization process.

Furthermore, the number of iterations to converge is an important parameter to take into account, as it gives an interpretation of the efficiency and stability of the selected approach. The less iterations, the more stable and efficient a selected approach is.

Convergence criteria	Units
Frequency	$\sigma \leq 0.01\%$
Discreteness	$M_{nd} \leq 5\%$

Table 3: Convergence criteria of the design cases.

The qualitative criteria cannot be measured and can be formulated as an observation made by the author based on his interpretation of the result. These observations are categorized as:

- Efficiency for practical applications describes the process of setting up a simulation and fine tuning. If an approach requires too much fine tuning of the parameters to work, it will probably not be worthwhile to use in practise.

- Problems encountered during the optimization process (e.g. convergence instability and localized eigenmodes). These problems are difficult to quantify, but they are easily found in the results of the optimization process. For example, grey areas are easily seen in the final result of the geometry representation. Or localized eigenmodes can be observed from the iteration history, where the objective fluctuates between a high eigenfrequency and a frequency close to zero.

Finally, the sensitivity and Heaviside filter will be compared to one another, where after the best performing design will be used for the density method comparison. The same goes for the level-set method. The best performing CSRBF will be chosen, which will represent the level-set method for the comparison. The iteration history of the chosen method will be shown for comparison.

5.3 Benchmarks

To compare the different optimization approaches, two different geometries of the design domain and various boundary conditions are proposed. These examples have a simple geometric representation, whereby the differences in design space are more distinct. The most frequently used design example in literature is a simply supported beam with a size ratio of $(8:1)$. This is represented in Figure 14. Additionally, two extra boundary conditions of this beam design example are used. Furthermore, two plate-like 3D design examples are used to extend the results of the comparison. These 3D plates are also used for the case study in Section 7.
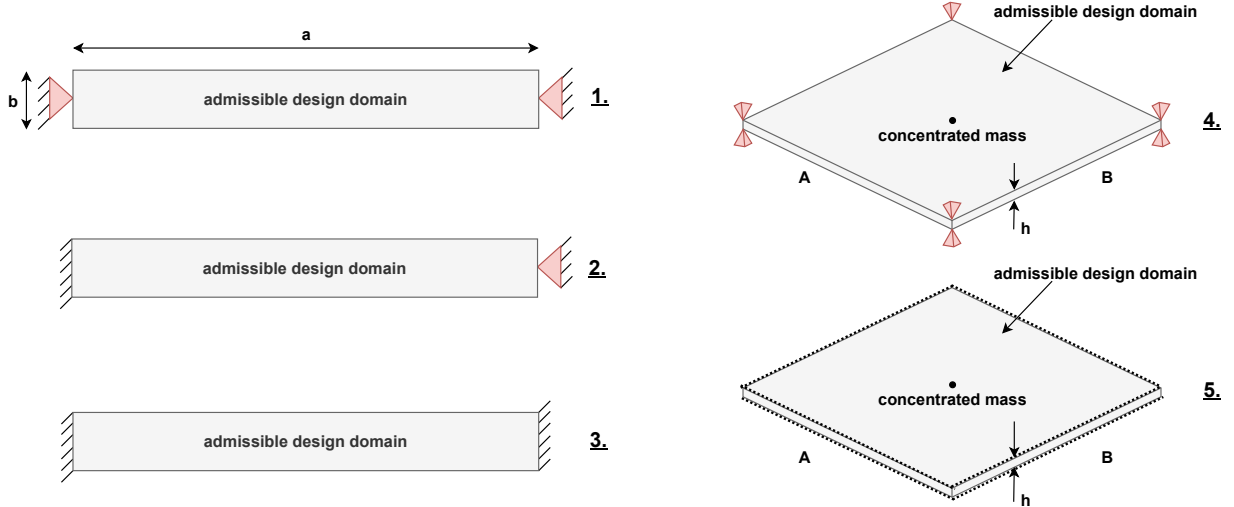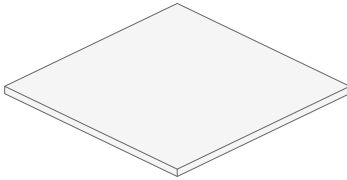
Figure 14: **1-3** Admissible design domain (a:b = 8:1) of a 2D plate like structure with plane stress elements and three sets of different boundary conditions. **1.** Simply supported at the ends. **2.** One end clamped and one end simply supported. **3.** Both ends clamped. **4-5** Admissible design domain of a plate like 3D structure (A:B:h = 1:1:0.01) with Mindlin-Reissner plate elements **4.** Simple support on the four corners and a concentrated mass at the centre of the plate of $M_c = M_0/10$ (M_0 is the total mass of the plate like structure). **5.** Same plate like structure, but the four edges are clamped. The concentrated mass is defined as $M_c = M_0/10$.

Parameter	Symbol	Unit		
Length	L	m	8	1
Width	W	m	1	1
X - elements	nelx	-	320	100
Y - elements	nely	-	40	100
Degrees of freedom	DOF	-	26,322	30,603
Thickness	h	m	-	0.01
Concentrated mass	M	kg	-	$M_0/10$
Volume fraction	V^*	%	50	50
Young modulus	E	Pa	1×10^7	1×10^7
Poison ratio	ν	-	0.3	0.3
Penalty	-	-	3	3
Density	ρ	kg/m^3	1	1

Table 4: Problem settings for the design examples.

5.4 Parameters settings

To make a distinct comparison between the density and level-set method, a regularization approach is implemented for the parameters (i.e. simplify the results by means of reducing the amount of adjustable parameters). Regularization is useful for a comparison, as it makes the amount of changeable parameters more concise. Consequently, the presented results may not be the most optimal, however it would be too time consuming to find the most optimal result for all of the design cases proposed for the comparison. The regularization results in two categories of parameters, which can be categorized into *problem settings* and *optimization parameters*.

- The problem settings are defined as design case specific parameters. They are independent for the comparison of the level-set and density method. Therefore, these parameters will be fixed throughout all the simulations of a given problem. The standard parameters with their corresponding value for the design examples are shown in Table 4.

- Optimization parameters are defined as method-specific parameters, which influence the optimization process in terms of e.g. convergence rate, simulation time and final result. They are different for the density and level-set approach. The goal of this work is not to compare these parameters to each other, rather if a design is unstable or can not converge due to these specific parameters, it will be adjusted for the given design case. The specific parameters are shown in Table 5.

  - *Continuation of β and ϕ_b*: The continuation of the β parameter in the Heaviside filter and the bandwidth ϕ_b in the level-set method play an important role in the convergence rate and design detail of the final design. The continuation should increase after a convergence criterion is met, which in this work is defined as $\sigma < \zeta$, or after a certain amount of iterations. The value for ζ is fixed throughout all simulations, however the criteria for amount of iterations can be changed depending on the design case to prevent instabilities. The incremental step for β and ϕ_b and their initial value is problem specific and must be tuned accordingly. In this work the starting value of $\beta = 1$ and a starting value of $\phi_b = 6$ elements. It is difficult to have these continuation strategies work in exactly the same sense, as the smoothened Heaviside approach works different compared to the bandwidth continuation approach. The bandwidth continuation is probably slower, due to the fully discrete design occurring when the bandwidth is $\phi_b = 1$, whereas the smoothened Heaviside approach could be discrete at an earlier continuation step.

Density method

Parameter	Filter radius	Initial β, η	Amount	Criterion [ζ]	Criterion [It.]	Remark
Sensitivity filter	r_{min} = 3	-	-	-	-	
Heaviside filter	r_{min} = 3	$\beta = 1$ $\eta = 0.5$	$\beta = \beta * 2$	$\sigma \leq 1\%$	Beam = 30 Plate = 40	

Level-set method

Parameter	Support radius	Initial ϕ_b	Amount	Criterion [ζ]	Criterion [It.]	Remark
C2	R = 6	ϕ_b = 6	$\phi_b = \phi_b - 2$	$\sigma \leq 1\%$	Beam = 30 Plate = 40	If ϕ_b is 2, final
C4	R = 6	ϕ_b = 6	$\phi_b = \phi_b - 2$	$\sigma \leq 1\%$	Beam = 30 Plate = 40	continuation step is ϕ_b = 1
C6	R = 6	ϕ_b = 6	$\phi_b = \phi_b - 2$	$\sigma \leq 1\%$	Beam = 30 Plate = 40	

Table 5: Optimization parameters for the optimization methods. The criterion columns are the update criteria for the continuation, where ζ is the difference in eigenfrequency and It. is the amount of iterations.

Furthermore, the initial design for the density and level-set are chosen to be the same. For the density method that is a design where each element has a density value equal to the specified volume fraction $V^* = 50\%$. The initial design input for the level-set approach is a zero level-set plane without any holes, which is equal to an initial design input of a volume fraction of $V^* = 50\%$. Most level-set approaches have an initial design input with holes, however the proposed level-set approach is able to produce holes over the whole design domain. Therefore, it was opted to not have an initial design input with holes.

6 Results of design cases

6.1 2D beam example with simply supported ends

In this section the results of the boundary condition of Figure 14.1 with maximization of the first eigenfrequency are presented. The parameters of Table 3, Table 4 and Table 5 are used. The results are shown in Table 6. From the results it is seen that the sensitivity and Heaviside filter have roughly the same performance in terms of objective function and M_{nd}. However, the Heaviside filter converges better due to its property of pushing element densities to either a void or solid state. Therefore, the Heaviside filter will be selected for the density representation. The level-set results from Table 6 show that the M_{nd} convergence criterion is met, furthermore the amount of iterations are roughly the same. However, there is a minor spread in the objective function. All the level-set designs have converged to a discrete design, where the higher order CSRBF perform best in this design case. The CSRBF 4 will be selected for the level-set representation. Although this result has one of the highest iterations, the objective function is highest compared to all designs.

This design case shows small deviations in the comparison criteria, but they are negligible. All of the designs have converged to a discrete design and to the same value of the objective function. There was no tuning needed for either of the techniques. Notably, the amount of iterations for the level-set method is slightly higher compared to the density method. This was expected, as the continuation strategy of the level-set bandwidth is slower than the Heaviside continuation, which is was expected (see Section 5.4).

An eigenfrequency iteration history of the design optimized using the density based approach is shown in Figure 15(a). The first and second eigenfrequency start as distinct eigenfrequencies, but during the optimization process they become multiple. The third eigenfrequency is also taken into account, so that the algorithm can distinguish the higher eigenfrequencies from the lower ones. The continuation of the β parameter does introduce some instability in the optimization process. At iteration 23 the eigenfrequencies dive down to a local eigenmode, causing some parts of the geometry to be isolated and resulting in localized eigenmodes. However, the solver seems to solve this problem in 4 incremental steps before the optimization process is stable again. Although this is an unwanted occurrence for the optimization process, it does not seem to interfere in the end result. Figure 15.(b) shows an iteration history for the level-set optimization. It can be seen that just like the density method the first two eigenmodes have multiplicity during the optimization process and the third eigenfrequency does not come to this eigenfrequency range. Interestingly, in contrast to the density results, the level-set results do not show the occurrence of localized eigenmodes. These results show similarities with the results in the work of Du and Olhoff [2007], which can be found in Appendix D.
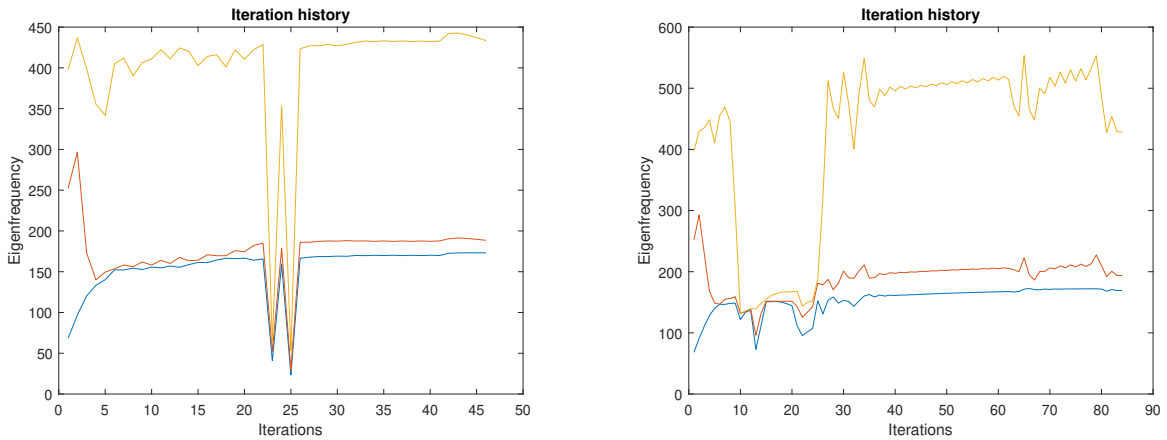
(a) Iteration history of a density optimization run with the Heaviside filter and a radius of 3 elements.

(b) Iteration history of a level-set optimization run with CSRBF 4 and 6 elements for the support radius.

Figure 15: Optimization runs of the density and level-set method for a simply supported beam.

Method	Optimized result	ω [rad/s]	M_{nd} [%]	Iterations
Density method				
Sensitivity filter		172.8	3.97	77
Heaviside filter		173.2	1.37	46
Level-set method				
CSRBF 2 (VF)		170.0	2.40	73
Zero level-set				
CSRBF 4 (VF)		174.5	0.80	84
Zero level-set				
CSRBF 6 (VF)		172.3	2.00	84
Zero level-set				

Table 6: Results for maximizing the first eigenfrequency of the beam with boundary conditions of 14.1. The methods with their corresponding numerical values are shown. The abbreviation (VF) refers to the Ersatz volume fraction of the level-set approach.

6.2   2D beam with maximization of bandgap between the second and third eigenfrequency

In this section the results of the 2D beam with boundary conditions of Figure 14.2 with a maximization of the bandgap between the second and third eigenfrequency is presented. The parameters of Table 3, Table 4 and Table 5 are used. The optimization converges when the condition $\sigma \leq 0.01\%$ is met, where σ is defined as the maximal relative difference of the second or third eigenfrequency as seen in Equation 44.

$$\sigma = max \left\{ \frac{|\lambda_{i+1}^2 - \lambda_i^2|}{\lambda_i^2}, \frac{|\lambda_{i+1}^3 - \lambda_i^3|}{\lambda_i^3} \right\} \tag{44}$$

In here i refers to the iteration number of the simulation. The results for this design problem are shown in Table 7. The sensitivity filter was unable to produce a design with a M_{nd} of less than 5%, therefore its stopping criterion of the M_{nd} is increased to 10% to be able to converge. Furthermore, the sensitivity and Heaviside filter again show practically similar performance, where the Heaviside filter outperforms the sensitivity filter in the amount of iterations and slightly outperformed in the M_{nd}. The sensitivity filter has a slightly better objective function, however it has more than 5% grey areas, making the results less significant. In terms of the final design representation, both of the filters seem to converge to the same

design. The Heaviside filter will be selected for the density representation.

The level-set results have considerable more deviation of the objective function compared to the density method. It is very likely the result of the implemented support radius, which is not optimal for this design case. This design example is rather difficult to solve for the level-set method, which resulted in the spread of the objective function. A possible cause is that the support radius is not optimal for this design case. Furthermore, the M_{nd} and iteration results are all rather similar. The CSRBF 6 will be selected for the level-set representation, as it has the highest ratio of the eigenfrequencies and needed the least amount of iterations.

The results show that the density method slightly outperformed the level-set method in terms of the objective function (4.6%) and amount of iterations (11 iterations). From the iteration history in Figure 16(a) it can be seen that the density method has a more stable convergence graph compared to the level-set method in Figure 16(b). However, the higher order frequencies (3rd and higher) have multiplicity in the density method, while the level-set method has no multiplicity in the higher order frequencies. Additionally, both the density and level-set approach did not have any problems with localized eigenmodes.

Unlike the density method, the level-set method needed additional tuning to have a more stable convergence. During the optimization process the level-set method had a tendency to disconnect on the thin parts at roughly one third and two third of the design domain. This was caused at the updated continuation step, which seemed to be too abrupt of an update step for this design case. Additional tuning of the algorithm was implemented to prevent this behaviour. In the previous design example (Section 6.1) the level-set method did not need any tuning, however this design case imposed some difficulties for the level-set method. This could be due to the support radius, which is may be not ideal for this design case. The density method did not impose this problem and had a more stable and faster convergence. Furthermore, in terms of discreteness, both methods seem to converge to a low value of the M_{nd}.
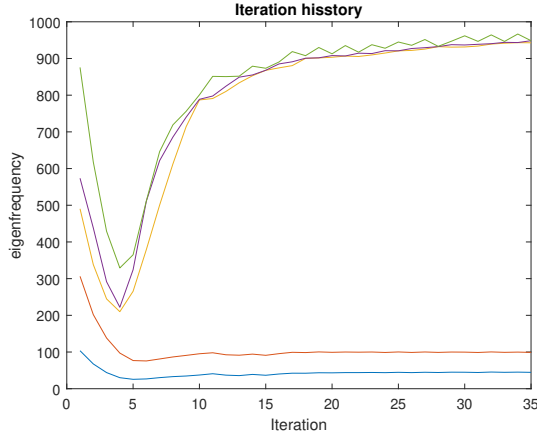
(a) Iteration history of a density optimization run with the Heaviside filter and a radius of 3 elements.
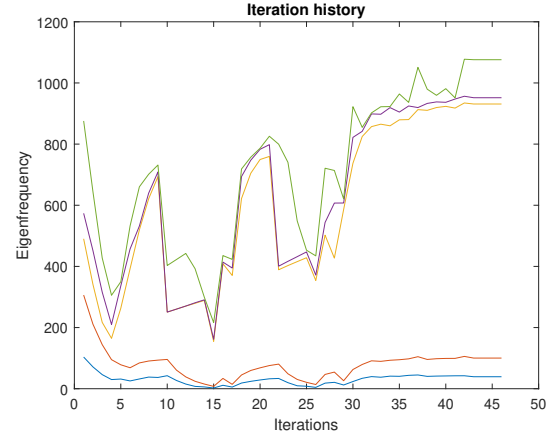
(b) Iteration history of a level-set optimization run with CSRBF 6 and 6 elements for the support radius.

Figure 16: Optimization runs of the density and level-set method for a beam with boundary conditions in 14.2

Method	Optimized result	ω_2/ω_3 [-]	M_{nd} [%]	Iterations
Density method				
Sensitivity filter		9.72	6.01	54
Heaviside filter		9.53	3.52	35
Level-set method				
CSRBF 2 (VF)		8.43	3.78	50
Zero level-set				
CSRBF 4 (VF)		8.90	1.41	58
Zero level-set				
CSRBF 6 (VF)		9.29	2.73	46
Zero level-set				

Table 7: Results for the bandgap objective function, where the separation of the second and third eigenfrequency must be maximized. The boundary condition of 14.2 is used. The methods with their corresponding numerical values are shown. The abbreviation (VF) refers to the Ersatz volume fraction of the level-set approach.

6.3   2D beam optimized for specific eigenfrequency

In this section the results of the 2D beam with boundary conditions of Figure 14.3 are presented. The beam is optimized for a specific eigenfrequency of $\omega_o = 300$ rad/s. The parameters of Table 3, Table 4 and Table 5 are used. There is one small change in the convergence criteria of the measure of discreteness, which is now $M_{nd} \leq 10\%$. The reason for this change is that this design case proved to be difficult to converge to a $M_{nd} \leq 5\%$. Therefore, the convergence criteria is increased to 10%.

The results for this design problem are shown in Table 8. The sensitivity filter shows a lot of grey areas and was not able to converge. As the sensitivity filter only modifies the sensitivities, it has difficulties to produce a discrete design in this design case. The filter is solely reliant on the penalization on the elements for discreteness, which in this design example tends to result in excessive grey areas. On the other hand, the Heaviside filter results in a crisp design representation and does converge due to the continuation. In terms of the comparison, the Heaviside filter outperforms the sensitivity filter on all criteria except on the objective function, although objective function of the sensitivity filter is marginally better. However, due to the substantially high M_{nd} value, this value can not be interpreted as a reliable end objective function. Therefore, the Heaviside filter is used for the comparison.
The continuation approach for the level-set method as described in Table 2.4.4 seems to result in convergence instabilities for this design case. These simulations revealed that this design case is non-convex to a

greater extend than previous design cases (Section 6.1 and 6.2). Therefore, the continuation strategy needs to be adjusted to obtain convergence. This adjustment is implemented in the form of an extra step between $\phi_b = 2$ and $\phi_b = 1$. An intermediate step of $\phi_b = 1.5$ elements is implemented to smoothen the continuation. Furthermore, the designs of the level-set method converge to different local minima. In the final design representation there is a considerable amount of grey areas present, which confirms the non-convexity of this objective function. Although the CSRBF 4 has a low M_{nd} value, the design representation has some complex geometric features that connect via grey elements. Moreover, the CSRBF 4 is significantly better compared to the CSRBF 2 and CSRBF 6 in terms of the comparison criteria. The CSRBF 6 is slightly better in the objective function. However, the M_{nd} is larger than 5%, resulting in an unreliable result for the objective function. To conclude, the CSRBF 4 results are used to represent the level-set approach for the comparison.

From the iteration history in Figure 17 it can be seen that both methods suffer from convergence instabilities during the optimization process. However, as the design becomes more discrete, the optimization stabilizes. In both the density and level-set method, the first and second eigenfrequency have multiplicity at the end of the optimization. The density method did suffer from localized eigenmodes at iteration 35, 38 and 47. However, this did not seem to cause any problems during the optimization. Furthermore, Table 8 show rather similar performances for the density and level-set approach in terms of the quantitative criteria. The level-set approach has a slightly better objective function and the density method has slightly better M_{nd} value and needed less iterations, but they are not substantial. Moreover, in terms of the qualitative criteria, the density method had a slight advantage over the level-set method in terms of tuning and the final geometric result. The continuation of the Heaviside filter is smoother per update step, whereas the level-set method has a more abrupt updating step. This update step of the level-set method needed extra tuning to converge with the proposed criteria. The final design representation of the density method is highly defined, whereas for the level-set method there are some geometric features that are connected via grey elements. The density method proved to be more efficient than the level-set method, however these results need to be interpreted with care. The objective function is non-convex to a great extent, which could favor the level-set approach for more complex design cases.

(a) Iteration history of a density optimization run with the Heaviside filter and a radius of 3 elements.

(b) Iteration history of a level-set optimization run with CSRBF 4 and 6 elements for the support radius.
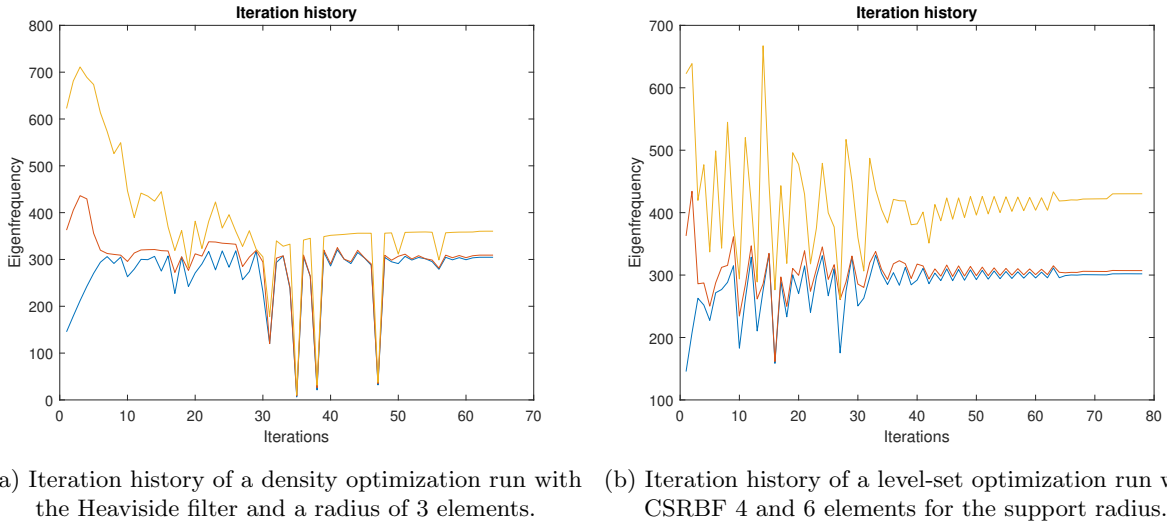
Figure 17: Optimization runs of the density and level-set method for obtaining a specific eigenfrequency of 300 rad/s. The geometry is a beam with the corresponding boundary conditions of Figure 14.3.

Method	Optimized result	ω [rad/s]	M_{nd} [%]	Iterations
	Density method			
Sensitivity filter		295.9	64.00	500
Heaviside filter		304.7	0.26	64
	Level-set method			
CSRBF 2 (VF)		295.7	8.03	253
Zero level-set				
CSRBF 4 (VF)		301.9	2.72	88
Zero level-set				
CSRBF 6 (VF)		300.4	6.11	103
Zero level-set				

Table 8: Results for obtaining an eigenfrequency of 300 rad/s with the boundary conditions of Figure 14.3. The abbreviation (VF) refers to the Ersatz volume fraction of the level-set approach.

6.4 3D plate structure with simply supported corners

In this section the results of the boundary condition of Figure 14.4 with maximization of the first eigenfrequency are presented. The parameters of Table 3, Table 4 and Table 5 are used. The results of this design example are shown in Table 17. The results show that the Heaviside filter is outperforming the sensitivity filter in terms of the M_{nd} and the total amount of iterations, whereas the objective function is practically the same. Although the final geometry representation converges to roughly the same local minimum, the Heaviside filter significantly outperforms the sensitivity filter. Therefore, the Heaviside filter will represent the density method for the comparison. The level-set method has comparable results in terms of the quantitative results. Only the CSRBF 2 needs more iterations before convergence compared to the other CSRBF. The objective function and M_{nd} have practically the same values. There is however one noticeable difference, which is the final design representation. Interestingly, each of the level-set method converges to a different local minimum. Although both the CSRBF 4 and CSRBF 6 results are suited for representing the level-set method in the comparison, it was opted to choose the CSRBF 4 due to less iterations before convergence. An iteration history is shown in Figure 18. In both of the simulations the second and third eigenfrequency are multiple from the beginning and throughout the simulation. The iteration history of both examples show no presence of localized eigenmodes and a stable convergence throughout the simulation. There is one small remark regarding efficiency. The level-set method is slightly more stable for this design case compared to the density method in terms of tuning. The level-set results did not need any tuning, whereas the density method did need some additional tuning of the algorithm. To conclude, both methods do not seem to encounter difficulties in this design case other than a marginally smaller M_{nd} value for the level-set approach.
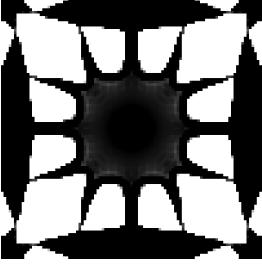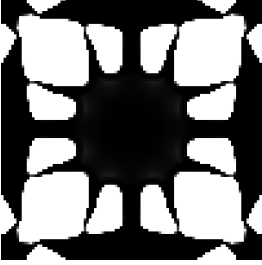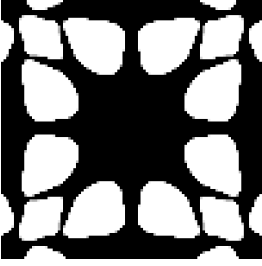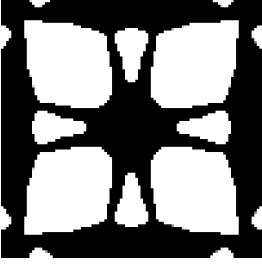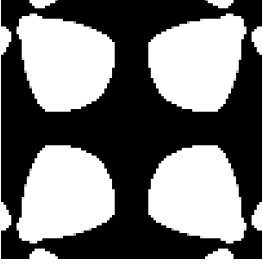
Method	Optimized result	ω [rad/s]	M_{nd} [%]	Iterations
Density method				
Sensitivity filter		75.9	5.00	340
Heaviside filter		75.6	2.93	43
Level-set method				
CSRBF 2 (VF)		75.8	1.31	75
CSRBF 4 (VF)		76.6	0.15	41
CSRBF 6 (VF)		76.3	0.22	56

Table 9: Results for maximizing the first eigenfrequency of the 3D plate with boundary conditions of 14.4. The methods with their corresponding numerical values are shown. The abbreviation (VF) refers to the Ersatz volume fraction of the level-set approach.
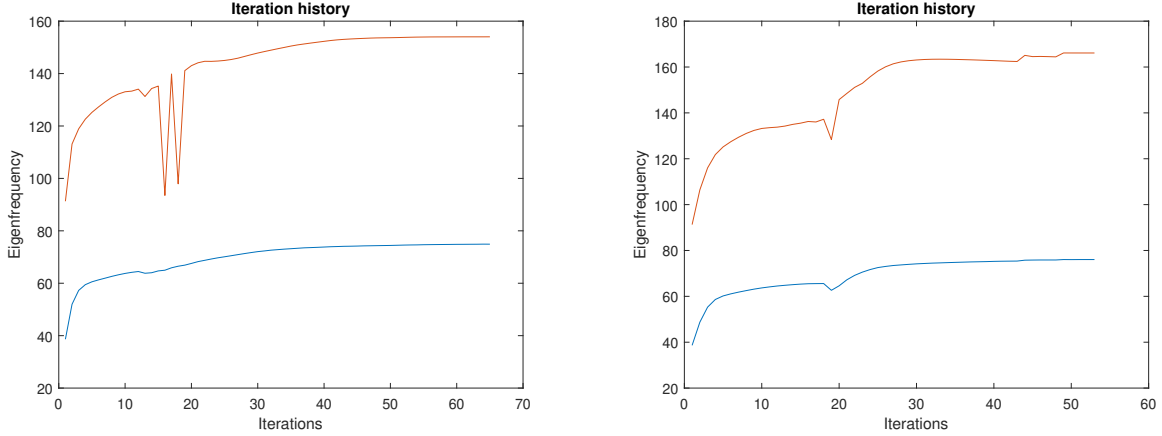
(a) Iteration history of a density optimization run with the Heaviside filter and a radius of 3 elements.

(b) Iteration history of a level-set optimization run with CSRBF 4 and 6 elements for the support radius.

Figure 18: Iteration history of the 3D plate, with simply supported ends. The second and third eigenfrequency are multiple in both examples from the beginning till the end.

6.5   3D plate with maximization of the second eigenfrequency

In this section the results of the boundary condition of Figure 14.4 with maximization of the second eigenfrequency are presented. The parameters of Table 3, Table 4 and Table 5 are used. The results are shown in Table 10. Remarkably, the sensitivity filter outperforms the Heaviside filter in this design example by a significant margin. The Heaviside filter need fewer iterations than the sensitivity filter, however it is insignificant as the objective function is significantly worse. The Heaviside filter has a tendency to create small geometric features that did not improve the objective function after the continuation. This is probably caused by the filter radius. Optimizing the filter radius for this design example could provide an improved solution, however this is out of the scope for the proposed comparison set-up. Nevertheless, the sensitivity filter outperforms the Heaviside filter and will represent the density method for the comparison.

The level-set method results show that the CSRBF 4 is outperforming the CSRBF 2 and CSRBF 6 in terms of the objective function and amount of iterations before convergence. It needs the least amount of iterations and has the highest objective function of the three methods. Remarkably, the final design of the CSRBF 4 and CSRBF 6 have rather different geometric features, but their objective function is practically the same. Additionally, all the level-set designs are unsymmetrical. This is probably caused as the second and third eigenmode are multiple from the beginning. These two eigenmodes have the same shape, however they are orthogonal in their direction. This multiplicity condition during the whole optimization process probably resulted in the unsymmetrical designs instead of a definite symmetric final design. Furthermore, the simulations show that the M_{nd} is very low on all CSRBF results (i.e. $M_{nd} \leq 1\%$). For the representation of the level-set method for the comparison the simulation of the CSRBF 4 is opted.

The iteration history of the sensitivity filter and the CSRBF 4 are shown in Figure 19. These two figures confirm that both the methods are stable for this design case. The second and third eigenfrequency are multiple from the beginning and throughout the simulation. Furthermore, the figures show that there are no localized eigenmodes occurring during the simulation. Both the density and level-set approach are stable in this design case and did not need additional tuning. Remarkably, the level-set method outperformed the density method on all quantitative criteria. Especially the objective function of the level-set method is significantly higher than the density method.
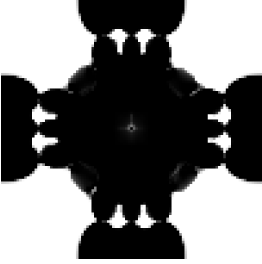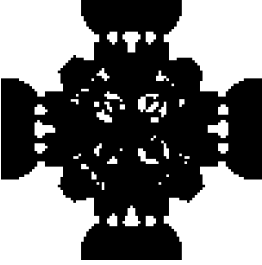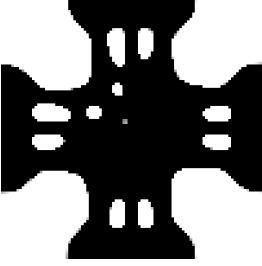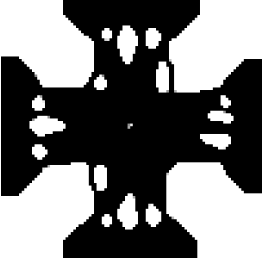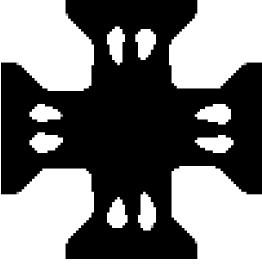
Method	Optimized result	ω [rad/s]	M_{nd} [%]	Iterations
Density method				
Sensitivity filter		701.9	3.63	75
Heaviside filter		650.0	0.01	65
Level-set method				
CSRBF 2 (VF)		738.2	0.41	92
CSRBF 4 (VF)		756.7	0.17	62
CSRBF 6 (VF)		755.1	0.07	92

Table 10: Results for maximizing the first eigenfrequency of the 3D plate with boundary conditions of 14.4. The methods with their corresponding numerical values are shown. The abbreviation (VF) refers to the Ersatz volume fraction of the level-set approach.
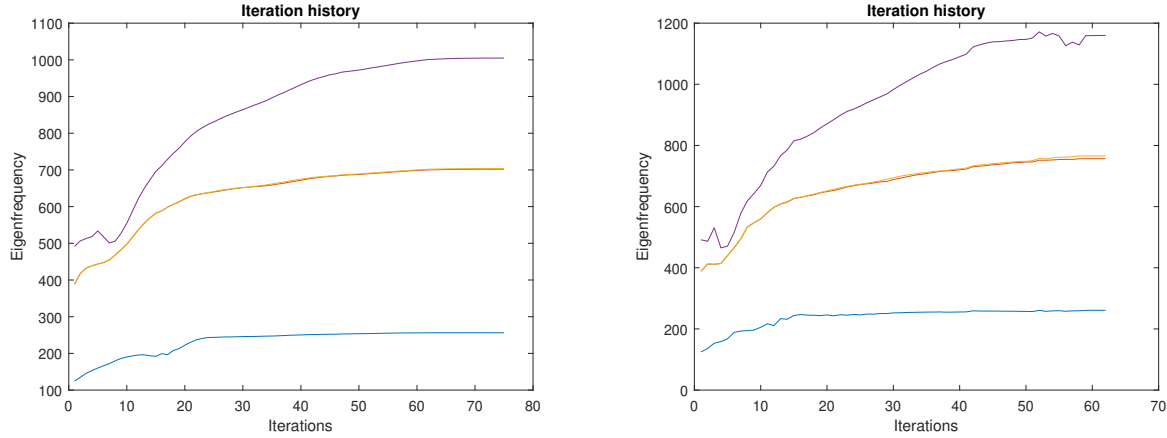
(a) Iteration history of a density optimization run with the sensitivity filter and a radius of 3 elements.

(b) Iteration history of a level-set optimization run with CSRBF 4 and 6 elements for the support radius.

Figure 19: Optimization runs of the density and level-set method for a 3D plate with maximization of the second eigenfrequency. The boundary condition of Figure 14.5 is used. The second and third eigenfrequency are multiple from the beginning and throughout the simulation.

6.6   Mesh size influence

To further investigate the performance of the density and the level-set methods, a parametric study with various mesh sizes is simulated. The design case for this comparison is the simply supported beam (boundary conditions 14.1) with maximization of the first eigenfrequency as objective function. To compare the performance in terms of number of iterations before convergence, several discretizations are proposed namely: 160×20, 320×40 and 640×80. Furthermore, all the values of Table 3, Table 4 and Table 5 are used, except for the discretization, the filter radius and the support radius. One study consists of a mesh-independence study, where the filter radii of the sensitivity and Heaviside filter are $r_{min} = [2, 4, 8]$ for increasing discretizations. This study should result in relatively consistent results. Furthermore, two additional studies are performed where the filter radius is fixed at $r_{min} = 2$ and $r_{min} = 4$ elements throughout the discretizations. This study is to show the influence of the filter radius on the various discretizations. Moreover, the level-set approach has one study where the support radii are 7 for the CSRBF 2, 5 for the CSRBF 4 and 3 for the CSRBF 6. This adjustment for the support radius has been implemented to have stability throughout the various discretizations. The results are shown in Table 11. The objective function, amount of iteration for convergence and the time per iteration is taken into account for the results. There are a few interesting observations that can be made based upon this design case.

Firstly, as the discretization increases, the objective function of both methods increases. The maximal and minimal values per method with its corresponding discretization is shown in Figure 20. The results highlight the importance of the discretization for the final result, as the worst performing (coarse mesh and level-set CSRBF 6) and best performing (fine mesh and level-set CSRBF 4) studies have a difference of 9.1%. Furthermore, the spread in each discretization is 4.5% for 160×20, 4.4% for 320×40 and 3.8% for 640×80, which are small spreads.

The results of the simulations in Table 11 show that the mesh-independent study of the density approach shows relatively consistent results over the various discretizations, as was expected. Furthermore, the Heaviside filter converges the fastest on a coarse discretization. Based on this observation it is slightly more preferred to use the Heaviside filter when a coarse discretization is to be simulated. On the other hand, the level-set method is slightly more preferred for finer discretizations in terms of the performance of the objective function. The simulations consumed twice as much iterations compared to the density method, however there are slightly more performance gains with the level-set approach. A possibility could be that the support radius of the level-set approach results in more detailed geometry elements, which in turn could results in an improved objective function. The density based study, where the filter radius is $r_{min} = 2$, should

	ω	T/It.	It.	M_{nd}	ω	T/It.	It.	M_{nd}	ω	T/It.	It.	M_{nd}
Density Ω_h	160×20, $[r_{min} = 2]$				320×40, $[r_{min} = 4]$				640×80, $[r_{min} = 8]$			
Sensitivity filter	170.8	0.55	105	4.25	171.6	1.15	57	5.00	171.8	4.80	65	4.79
Heaviside filter	**170.9**	0.49	38	0.02	172.6	1.54	52	0.01	173.4	5.82	51	0.01
Density $[r_{min} = 4]$ Ω_h	160×20				320×40				640×80			
Sensitivity filter	164.3	0.36	206	4.91	171.6	1.15	57	5.00	175.0	5.14	64	4.26
Heaviside filter	163.8	0.52	50	0.02	172.6	1.54	52	0.01	175.4	5.51	46	0.01
Density $[r_{min} = 2]$ Ω_h	160×20				320×40				640×80			
Sensitivity filter	170.8	0.55	105	4.25	170.6	1.35	44	4.90	**176.1**	6.53	46	4.05
Heaviside filter	**170.9**	0.49	38	0.02	**174.2**	2.67	48	0.01	175.8	5.65	41	0.01
Level-set Ω_h	160×20				320×40				640×80			
CSRBF 2, [R = 7]	163.8	0.41	112	3.06	166.8	1.68	118	3.75	175.0	5.16	83	1.53
CSRBF 4, [R = 5]	**168.4**	0.35	121	1.29	173.8	2.46	100	1.36	**178.4**	6.54	76	0.40
CSRBF 6, [R = 4]	163.5	0.34	218	3.79	**174.6**	1.48	76	1.14	176.6	5.96	95	1.23

Table 11: Comparison of numerical performance of the density and level-set method. The value It. represents the amount of iterations for convergence. The value r_{min} is the filter radius for the sensitivity and Heaviside filter. The value R is the support radius for the CSRBF. The value T/It. represents the simulation time per iteration in seconds, Ω_h represents the discretization, the value ω is the objective function in rad/s and the M_{nd} value is in percent.
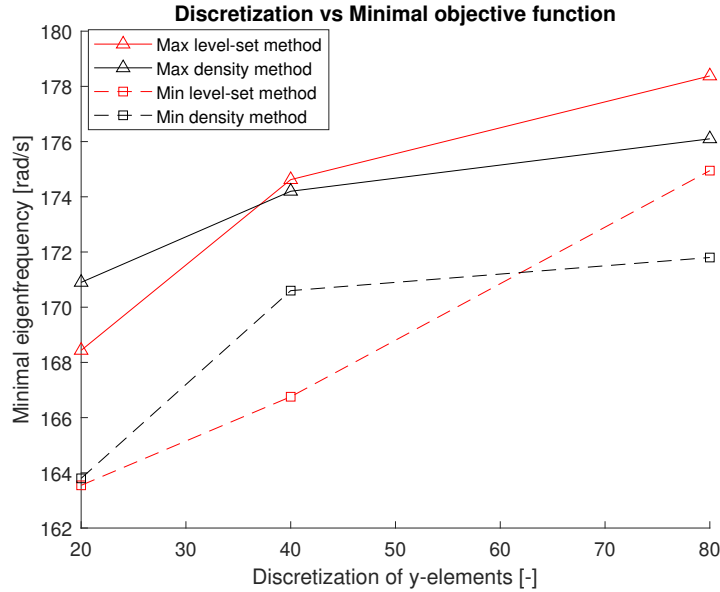
Figure 20: Minimal and maximal values of the results shown in Table 11. A larger discretization results in an improved trend of the objective function.

(a) Heaviside filter result with $\omega = 173.4$, $r_{min} = 8$ and a discretization of 640×80.

(b) Heaviside filter result with $\omega = 175.4$, $r_{min} = 4$ and a discretization of 640×80.

(c) Sensitivity filter result with $\omega = 176.1$, $r_{min} = 2$ and a discretization of 640×80.

(d) CSRBF 4 volume fraction result with $\omega = 178.4$, R = 5 and a discretization of 640×80.
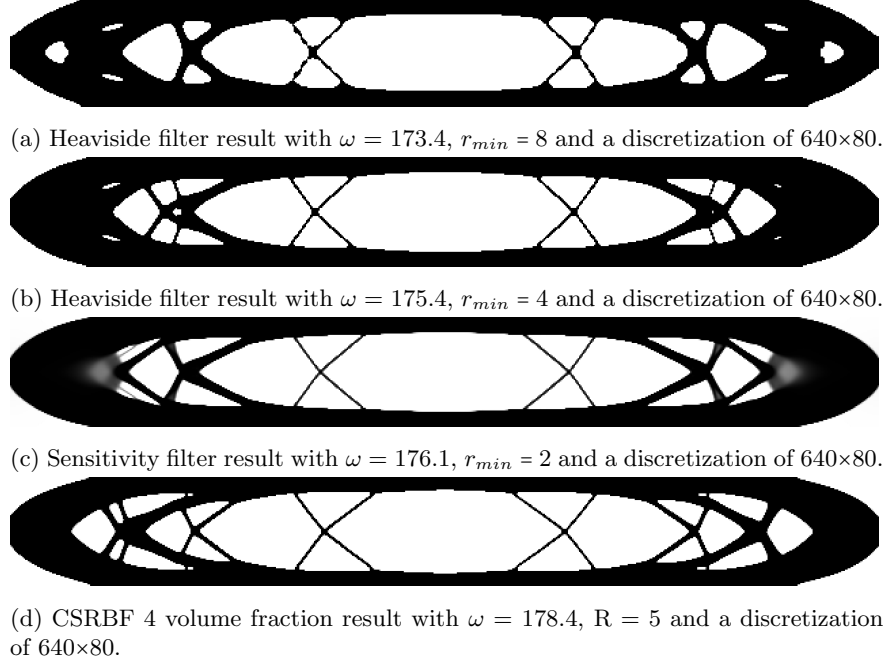
Figure 21: Final design representation of smallest mesh size of results in Table 11.

result in the best performing designs, as the most detailed design presentation can be found. However, it was not able to outperform the level-set approach. To add to that, the support radii for the level-set approach are not optimized for this design case, so it is possible there is still some performance to be gained for the level-set approach. The final results of the smallest mesh size with their corresponding best result are shown in Figure 21. These figures show that the filter radius of 8 elements results in less design detail. The filter radius of 4 elements does result in more detailed geometry elements and the filter radius of 2 elements results in the most detailed geometry representation. The level-set result also shows a considerable amount of detailed geometry elements and has some similarities with the filter radius of $r_{min} = 2$ and $r_{min} = 4$ elements. Furthermore, the total amount of iterations decreased for the level-set approach as the discretization increases, whereas the density method was relatively consistent in the amount of iterations over the various discretizations. As expected, there is a positive correlation in the amount of time per iteration for larger discretization. However, the level-set method needs slightly more time per iteration compared to the density method for larger discretizations. This is probably caused by the mapping of the level-set function from the elements to the nodes. Also, it could be caused due to additional multiplicity accidentally occurring during the simulation. This causes longer computation times per iteration as additional eigenvalue computations need to be calculated to compute the sensitivity during multiplicity (as explained in Section 3.3.2). Although the time per iteration ramps up higher for the level-set method, it is not significantly different compared to the density approach.

It must be noted that, as in previous design cases, the continuation of the level-set method is slightly slower compared to the continuation of the Heaviside filter. Therefore, the amount of iterations is probably higher compared to the Heaviside filter due to this continuation strategy. Furthermore, the support and filter radius are not optimized for each discretization. This causes non-optimal result for this design study. However, the goal of this study is to show the response to an increased discretization without any tuning of the parameters. To conclude, this study showed that the density approach is slightly more favored for a coarse mesh and the level-set approach is slightly more favored for a fine mesh. However, the differences are minor and no significant conclusion can be drawn from these results.

6.7   Discussion

From the design cases it is clear that the Heaviside filter for the density approach and the CSRBF 4 for the level-set approach resulted in the best performing designs. A better overview of both of these approaches and their results can be found in Appendix A.

6.7.1   Density method

The density approach is implemented with the use of the modified SIMP method combined with the sensitivity filter and the Heaviside filter. The modified SIMP method did sometimes result in the occurrence of localized eigenmodes. Although these localized eigenmodes occurred during an optimization run, they were not a substantial problem in the convergence process.

The sensitivity filter is frequently used in literature as it is easy to set-up and limited tuning is needed. However, the filter is often considered as heuristic and inconsistent for filtering, because the sensitivities are blurred and inconsistent to the objective function. Nonetheless, due to the penalization power used in this work ($p = 3$), the sensitivity filter is able to produce discrete designs ($M_{nd} \leq 10\%$) up to a certain degree. To supplement the density method with an additional design representation, a Heaviside filter is added. This filter provides consistent sensitivity information and, due to the Heaviside function, is better equipped to produce discrete designs. This filter has the possibility to tune the update step of the β parameter, giving more flexibility for the non-linear vibration problems. Furthermore, the Heaviside filter resulted in a relatively quick convergence of the design cases. It was expected that it would outperform the sensitivity filter, as a convergence criterion is the M_{nd} value, which is easier for the Heaviside filter to obtain. Also, it was marginally faster than the level-set approach is most design cases. Although this looks like a promising advantage of the Heaviside filter, it was probably the result of the chosen continuation strategy that resulted in this speed up of the convergence. Therefore, this speed-up should be interpreted with care.

A drawback of the density method is that it is slightly more prone to converge to a poorer local minimum compared to the level-set method. This could be caused due to the filter radius, however in the mesh study of Section 6.6 the smallest filter radius was not able to outperform the level-set approach. Even though the difference is minor, it was a small noticeable difference from all the design cases. Furthermore, the occurrence of localized eigenmodes is still possible, even though the modified SIMP should prevent this. Remarkably, these local eigenmodes only occurred in the 2D cases and not in the 3D cases. It is not clear if this is related to the FEM formulation, design cases or just coincidence that it did not occur at the 3D cases. Although the occurrence of local eigenmodes can occur during a simulation, it did not cause problems for the convergence of the final result.

In general, the density approach is a versatile method that solves a wide variety of problems, with acceptable performance and without much tuning. The results from Section 6.6 showed that the density method is more preferred for simulations with a coarse mesh size compared to the level-set approach. The density approach needs significantly less iterations and a slightly more improved objective function of 1.5% is found for a coarse mesh size. However, as only one design case is tested for these results, the recommendation should be interpreted with care.

From an industrial point of view, the technique is user-friendly, easier to grasp and implement. This characteristic is useful, as not every user has a full understanding of topology optimization. It could be argued that someone needs training before the use of topology optimization. However, it is becoming more readily available in various software packages, therefore a robust and easy to understand method is preferred in this area. A downside from the density method is that the final design representation is dependent on the discretization. A coarse mesh results in a coarse geometry description and is therefore more difficult to replicate in a computer aided design (CAD) environment. From an academic point of view, the density approach is easy to set up, widely studied and most state of the art research is based upon the density approach [Zargham et al., 2016]. Well-performing results can easily be achieved with large mesh sizes and little amount of iterations.

6.7.2   Level-set method

Level-set based topology optimization entails a broad range of methods to solve a topology optimisation problem. Three key aspects from the level-set approach can be categorized as: mechanical model, parameterization and optimization strategy. To have a fair comparison between the density method and the level-set method, keeping as many similarities between the two methods as possible is desired. Therefore, material parameter sensitivities in combination with MMA is used to update the design variables. Furthermore, a density-based geometry mapping is applied. This update strategy together with the mapping results in an almost similar structure as the density approach. The key difference lies in the parameterization of the level-set function, where the CSRBF have been used. These functions span a mid-range area providing a balance between design detail, memory allocation and convergence rate. Additionally, it is wished that there is some variation in the design representation to minimize the influence of the fixed parameters. Therefore, 3 types of CSRBF have been considered to showcase various design representations.

Furthermore, most level-set approaches are supplied with an initial design that include holes at various locations. The boundaries of these holes can be tracked by the level-set approach, which in turn change the geometry. A disadvantage of tracking the boundaries is that new holes can not be nucleated in the geometry. Regularization techniques need to be implemented to produce new holes in the geometry, which could comprise the rate of convergence of the optimization process. Moreover, the final design becomes more sensitive to its initial design and parameter input. In this work the level-set approach does not track the moving boundaries, rather it uses the material parameter sensitivity information of the whole design domain. This proves to be useful for producing new holes in the geometry, as sensitivity information of the whole design domain is used. Moreover, the method is not dependent on an initial design with holes, rather it can be a flat level-set surface. Thus it is less sensitive for the initial design input and no regularization is needed for nucleating new holes.

A limitation of the implemented level-set approach is the construction of the connectivity matrix (see Section 4.1.1). This matrix maps the density design variables to the level-set design variables (i.e. the element values are mapped to the nodes for the level-set function). Even though this is a sparse matrix, it consist of $M \times N$ (M = mesh elements) (N = nodes) matrix elements. Consequently, this matrix allocates a considerable amount of computer memory and the construction of this matrix consumes a considerable amount of computation time. There are probably more efficient ways to construct this connectivity matrix, which have not been explored in this work. Another limitation from the level-set approach is that imposing a length scale is less straightforward compared to the density approach. In Andreasen et al. [2020] this length scale control of the level-set approach has been investigated, however this has not been implemented in this work.

The results from Section 6.6 show that the level-set approach works increasingly better with a finer mesh compared to the density method. The objective function and total amount of iterations decrease with a finer mesh. Other mapping methods could provide better results with a coarse mesh as shown in Villanueva and Maute [2014], however this has not been tested in this work. Interestingly, the total time per iteration is marginally larger compared to the density method. The average time per iteration for the density approach for the fine mesh is 5.58 seconds per iterations, whereas for the level-set approach it is 5.89 seconds per iteration, which is marginally larger. Remarkably, if the average time per iteration of the study with a filter radius of r_{min} = 2 is taken, the average time per iteration is 6.09 seconds per iteration, which is even larger than the level-set average time per iteration. It is probable that the density method suffered from more multiplicity than the level-set approach during the simulations, which consequently increased the time per iteration.

In general, the level-set approach is able to solve various vibration problems with the possibility to outperform the density method by the proposed criteria. The method also did not encounter the occurrence of localized eigenmodes, making this method more stable than the density method. Some simulations look unstable due to the rapid change of the eigenvalues. However this is probably caused by the continuation step of two elements, which could result in these rigorous eigenvalue changes.

From an industrial point of view, the level-set approach comprises more tuning possibilities (e.g. support radius, CSRBF type, level-set input function, etc), to find the most optimal solution. However, the user requires more understanding of the influence of the level-set specific parameters. Furthermore, an advantage of the level-set approach is that it has a crisp geometry representation via the zero level-set plane. This design representation is more convenient to replicate the obtained design in a CAD environment compared

to the mesh element design representation of the density method. From an academic point of view, the level-set approach is able to achieve more performance at the cost of possibly more tuning time to find the optimal parameter settings. For example, finding the optimal support radius for the corresponding CSRBF is an experimental trial and error process [Buhmann, 2000]. As most academic literature is more focused on achieving the most optimal result for the presented method, the level-set approach is well-suited to achieve this objective.

6.7.3   Limitations of the benchmarks

These benchmark cases give an insight in the results for the density and level-set approach and their respective settings. Although several design cases are presented each with a different objective function, there is a difficulty in comparing two different methods. There are many variables that play a role in the final result, which could all be optimized per design case. This is the upside as well as the downside of optimization. On one hand it provides the possibility to optimize every variable to come as close as possible to the global optimum. On the other hand, from a comparison perspective, it would result in extensive simulations to find the most optimal values. Therefore, some limitations are introduced due to the comparison strategy proposed in this work.

- First of all, the most important limitation is the difficulty in comparing two methods that have different parameters (e.g. design variables, support radius, filter radius). To develop a representative comparison, it is wished that all the parameters are fixed throughout all simulations. This is unfortunately not possible for all design cases, as it results in instabilities in the optimization process. Therefore, a distinction between problem settings and optimization parameters is proposed. Only the optimization parameters are slightly adjusted in the case of convergence problems for the optimized design case. Although this strategy results in a meticulous approach that highlights the results of both methods, it is likely that the performance of the solvers is affected and consequently does not represent the full potential of both methods. Additionally, the support radius and the filter radius do not have the same length scale implemented. This may lead to different objective results. A solution to this problem is proposed by Andreasen et al. [2020], however this has not been implemented in this thesis.

- Furthermore, the design cases consist of simple geometric design domains and the structural analysis is done via simple plane stress quadrilateral elements. Although more variety is implemented via the use of Mindlin-Reissner plate elements, it does not encompass the performance difference for more complicated design cases and a more comprehensive FE structural analysis.

- Moreover, given that the performance study of Section 6.6 is based on one design case, the results regarding this simulation should be interpreted with care. In this design case it became clear that a finer mesh favors the level-set approach slightly more and a coarse mesh favors the density approach slightly more. However, as only one design case has been tested, it does not give a definitive recommendation for all design cases. Not only the single sample size is a limiting factor, also the implemented quadrilateral plane stress mesh elements could produce an error in the results for a coarse mesh discretization for both methods.

- Finally, MMA is well suited to solve the optimization problems for the density and the level-set approach. However, both methods were sometimes prone to numerical oscillations. These oscillations are probably caused by MMA due to its monotonicity property [Rojas-Labanda and Stolpe, 2015]. Therefore, the GCMMA can provide a solution for these oscillations, however it can have problems with its convergence. To remedy these problems, Zuo et al. [2007] proposed a hybrid algorithm consisting of MMA and GCMMA, which could help in the convergence.

7   Spring problem

As presented in the introduction, a design case of an out of plane membrane spring will be studied as a design case to demonstrate the applicability of the presented approaches. The spring is subjected to an harmonic external force that excites the spring in the out of plane direction. It is desired that the spring has the same frequency as the driving frequency of the external force, as this makes the machine more energy efficient, resulting in a smaller external motor and thus an overall compacter and lighter design. An example of the actuator is shown in Figure 22. The overall optimization objectives and constraints are:

- Synthesize desired first out of plane eigenfrequency of f_1 = 12.5Hz.

- Material properties of stainless steel (SS 301) are used for its fatigue strength.

- Mass of the actuator is 0.4 kg.

- The diameter of the spring is 60 mm and the thickness of the spring is 0.6 mm.

- The design should be as light as possible without sacrificing structural integrity.

- Increase higher order eigenfrequencies by a factor 2 of the synthesized eigenfrequency, so that multiplicity is avoided. This is shown in Equation 45, where f_i is the eigenfrequency of order i and J is the maximal amount of eigenfrequencies to be considered for this problem.

$$f_i > 2 * f_1, \qquad i = 2, 3, ..., J. \tag{45}$$

7.1   Modeling approach

The objective function of this spring example is to synthesize the first eigenmode at an eigenfrequency of 12.5 Hz. The first eigenmode of the spring is an out of plane mode as shown in Figure 24a. This is also
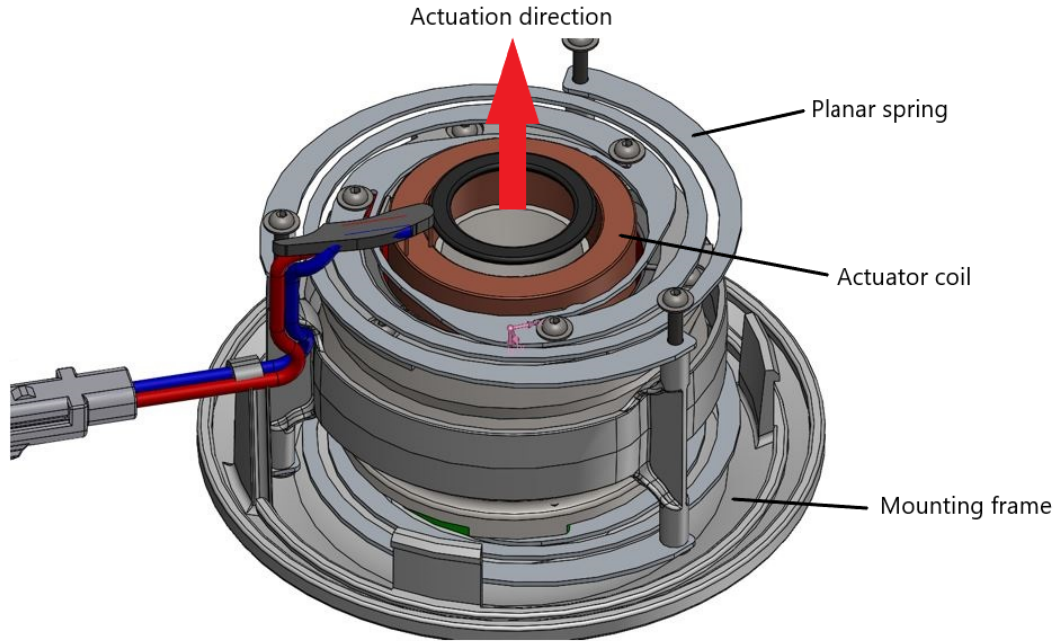
Figure 22: Planar spring with actuator housing from Demcon [2021]

the movement that is excited by the actuator. To prevent other modes from occurring during actuation it is wished that the higher order modes should not become multiple with the first eigenfrequency. Therefore, additional constraints of maximizing the higher order frequencies are incorporated. The mathematical description of the objective function is defined as:

$$
\min_{\beta, \rho_1, .., \rho_N} \left\{ \frac{(\lambda_1 - \lambda_o)^2}{\lambda_o^2} + 0.1 * \frac{\sum_{e=1}^{N_E} \rho_e V_e}{V_0} \right\}, \tag{46a}
$$

$$
\text{Constraints}: \quad \beta - \lambda_j \leq 0, \qquad\qquad j = 2, .., J, \tag{46b}
$$

$$
\text{s.t.}: \quad \mathbf{K}\phi_j = \lambda_j \mathbf{M}\phi_j, \qquad\qquad j = 1, .., J, \tag{46c}
$$

$$
\phi_j^T \mathbf{M}\phi_k = \delta_{jk}, \qquad j \geq k, \quad k, j = 1, .., J, \tag{46d}
$$

$$
0 < \rho_{min} \leq \rho_e \leq 1, \qquad\qquad e = 1, 2, ..., N_e. \tag{46e}
$$

The volume constraint is less important for this design case. However, without this constraint, there is a tendency to produce unwanted geometry elements that do not contribute to the objective. To remedy this, a multi-objective function is implemented, where a small volume penalty term is added in the objective function. This term removes unnecessary geometry elements. A small value of 0.1 is used for the weight factor. Furthermore, the convergence criteria are listed in Table 12.

Convergence criteria	Units
Frequency	$\sigma \leq 0.05\%$
Discreteness	$M_{nd} \leq 5\%$

Table 12: Convergence criteria for the Chest Master design case.
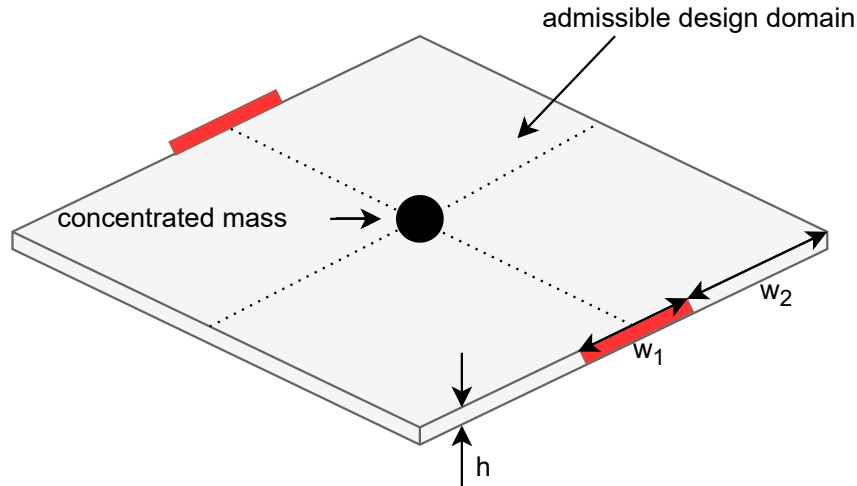
Figure 23: Boundary condition for the out of plane spring. The red side area is fully constrained (i.e. the line indicated by w_1). The location of the boundary conditions are defined by $W_1 = 6mm$ and $W_2 = 27$ mm. A concentrated mass at the centre of the plate of $M_c = 0.4$ kg. The center of the concentrated mass is defined in the center of the plate with a radius of r = 5 mm.
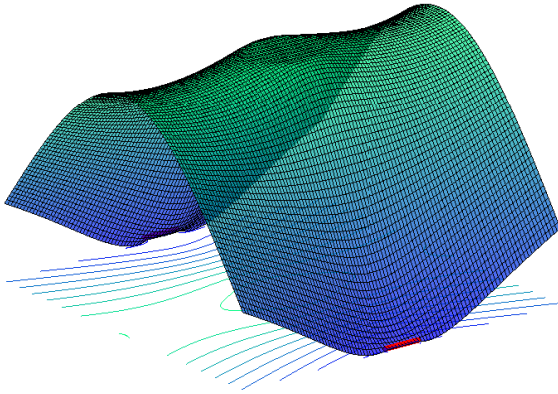
(a) First eigenmode Matlab 29.58 Hz
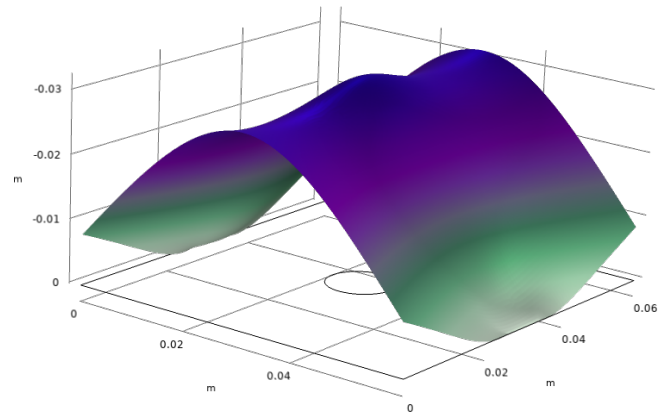
(b) First eigenmode Comsol 27.309 Hz
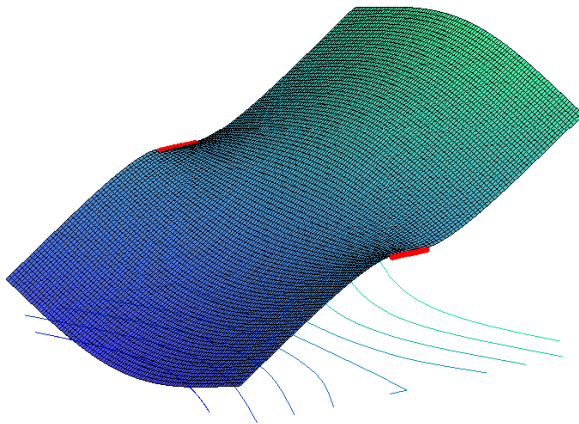
(c) Second eigenmode Matlab 82.04 Hz
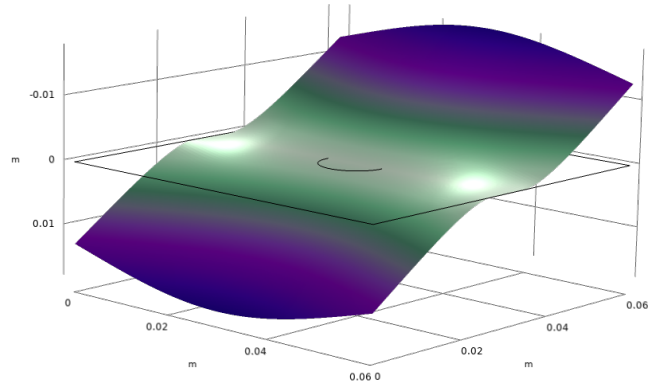
(d) Second eigenmode Comsol 84.585 Hz

Figure 24: First two eigenmodes for a fully solid plate with the presented boundary conditions. The red dots show the boundary condition as explained in Figure 23.

Model	1st eigenfrequency	2nd eigenfrequency
Matlab	29.58 Hz	82.04 Hz
Comsol	27.31 Hz	84.59 Hz
Difference	8.3%	3.1%

Table 13: Eigenfrequency values of the Matlab simulation and the Comsol simulation.

The boundary condition used for simulating the spring is shown in Figure 23. The boundary conditions are two fully constrained sides, defined by the red lines. The boundary conditions of Figure 23 are different from the representation in Figure 22, as the placement of the boundary conditions are free to choose for this design case. The material properties of stainless steel SS301 are a Young's modulus of $E = 200$ GPa, a density of $\rho = 8000$ kg/m^3 and a Poisson's ratio of $\nu = 0.3$. Furthermore, the dimension of the plate

is 60x60x0.6 mm and the discretization is 100x100 Reissner-Mindlin plate elements, which is simulated in Matlab. A concentrated mass in the center of the plate of 0.4 kg is added to simulate the actuator. This mass is spread across a ring of a radius of r = 5 mm. Moreover, the density with Heaviside filter and the level-set with CSRBF 4 will be used to solve this problem. There are two different studies that are simulated for this problem, as they produced the most optimal results for the design cases in Section 5. The following optimization strategy is adopted:

- Firstly, the density and level-set approach will evaluate this design case with the parameters used in previous design cases in this thesis, i.e. the values from Table 3 and Table 5. This study is intended to simulate this design case for someone that solves this design case in an industrial environment (i.e. with minimal adjustment of method specific parameters).

- Secondly, the design case is fully optimized for all method specific parameters by means of adjusting the continuation settings, support and filter radius and algorithm settings. This is to find the ultimate performance of both methods.

The initial two eigenfrequencies for a fully solid domain are verified in Comsol. The results are shown in Table 13 and their corresponding eigenmodes are shown in Figure 24. There is a slight difference of the Comsol model to the Matlab model, which is probably caused due to a difference in the discretization of the Comsol model and a difference in the definition of the concentrated mass.

7.2   Results with method specific settings from Section 5

The results of this section reflect the implementation in an industrial setting, where the method specific settings in Section 5 are used. The resulting designs for the density approach with Heaviside filter and the level-set approach with the use of CSRBF 4 are shown in Table 14 and in Figure 25. It must be noted that Figure 25.b shows a failed attempt of the density method. The iteration for both methods is shown in Figure 27.

Function	1st eigenfrequency [Hz]	2nd eigenfrequency [Hz]	M_{nd} [%]	Iterations
Density	10.22	54.16	0.08	86
Level-set	14.90	46.62	0.48	68

Table 14: Case study results with the use of parameters from Section 5.

Interestingly, both the methods diverged to a different final design. The density approach has considerably more material compared to the level-set approach. The density representation has a small disconnection in the top right part of the design. This in turn results in twisted eigenmode, which can be seen in Figure 26a. On the other hand, the level-set result does have the correct out of plane direction for the first eigenmode, as seen in Figure 26b. Furthermore, both methods have converged to a value of 10.22 Hz for the density method, having an offset of 18.2%, and 14.90 Hz for the level-set method, having an offset of 19.2 %. This is a considerable error for both methods for the desired eigenfrequency. Although the first eigenfrequency has a considerable error for both methods, the second eigenfrequency of both methods are well above the criterion of $2 \times f_0$. Also, the value for the M_{nd} is well below 5% for both methods. What is surprising is that the density approach had difficulties to converge in this design case, so some modifications to the algorithms were implemented to ensure a feasible result. A failed result can be seen in Figure 25.b. On the other hand, the level-set approach did not have any difficulties in this design case and converged without any problems. To conclude, the density representation is not suited for production, as it does have a considerable error in the objective function. Also, due to the disconnected part in the top right corner of the geometry, the direction of the eigenmode is changed, which makes it unsuited for this application. On the other hand, the level-set results also has a considerable error in the objective function. Therefore, the design is not optimal to use in a practical application. However, the final design is better suited to use in a practical application compared to the density approach, as the eigenmode has the right out of plane direction.

(a) Density approach representation.

(b) Failed density approach representation.

(c) CSRBF 4 density representation.

(d) CSRBF 4 zero level-set representation.

Figure 25: Results for the first case with the use of parameters from Section 5. The density method had difficulties to converge for this design case, so a failed convergence has been added in Figure (b).
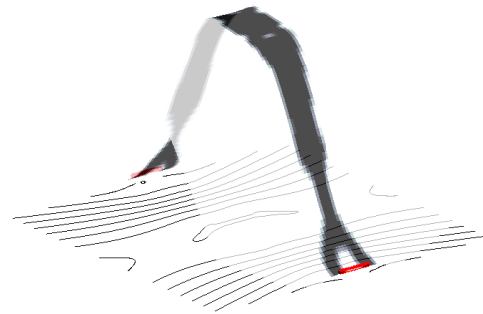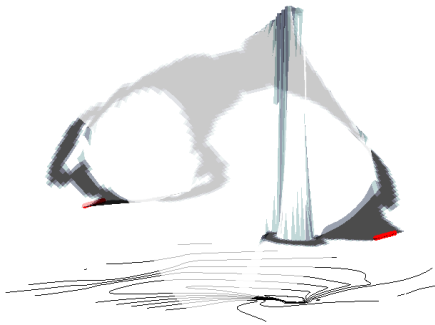
(a) First eigenmode of the density approach of 10.22 Hz, where the disconnected part results in a hinged eigenmodes.

(b) First eigenmode of the level-set approach of 14.90 Hz, with a good out of plane direction.

Figure 26: Results for the first eigenmodes of the results from the optimization run with the same method specific settings from Section 5. The red lines indicate the boundary condition of the plate.

(a) Iteration history of the density optimization run with a filter radius of 3 elements.

(b) Iteration history of the level-set optimization run with 6 elements for the support radius.
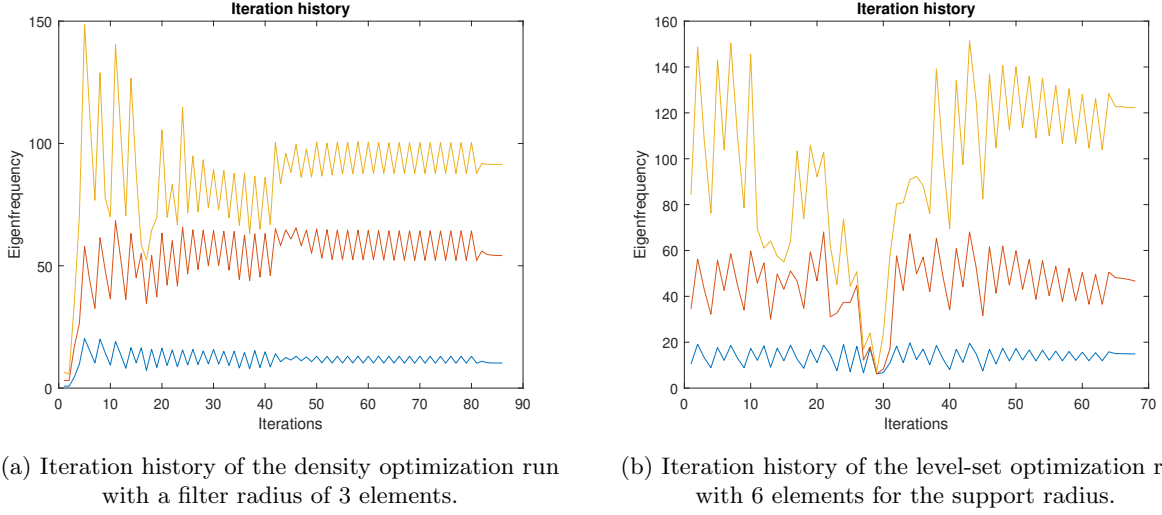
Figure 27: Optimization runs of the density and level-set method for the first study of the Chest Master spring.

7.3   Results with optimized settings

For this design case both the density and level-set methods are optimized for the most optimal performance. For the Heaviside filter the filter radius has been set to $r_{min} = 2$ to have the smallest length scale. Furthermore, the support radius for the level-set approach has been found experimentally, where a support radius of 5 elements seem to result in the best performing designs. The next step is to modify the continuation settings for both methods. The Heaviside filter continuation updates after 20 iterations with a factor of $\beta = \beta * 1.5$. The bandwidth continuation is set to an update step of $\phi_b = \phi_b - 0.04$ elements after every iteration, starting at 20 iterations. It was opted for these continuation strategies, as large continuation steps would result in instabilities in fast changing design changes. Due to the small incremental steps, the algorithm has time to alter the design for the most optimal solution. The results for the optimized settings are shown in Figure 28 and Table 15. A validation of the correct eigenmodes is shown in Figure 29, which shows the first and second eigenmode of both the density and level-set approach. The iteration history for both methods is shown in Figure 30.

Some general observations can be made from these results. First of all, both the density and level-set approach have similar design representations as in the first study of this design case in Section 7.2. Furthermore, the results in Table 15 show that the first eigenfrequency now has an error of 0.08 % for both methods, which is almost a negligible difference. The second eigenfrequency however is substantially larger for the density approach compared to the level-set approach. Even though it is advantageous to have a higher second eigenfrequency, the requirement of $f_i > 2 * f_1$ is met for both cases. Finally, both of these results seem feasible from a manufacturing perspective. The preference lies in difference between a more simple and lightweight design, for the level-set approach, over an increased second order eigenmode for the density approach.

To conclude, both methods seem feasible to be used in a practical application. The objective of synthesizing the first eigenfrequency at 12.5 Hz is achieved with an error of 0.08%. The difference lies in a more improved second eigenfrequency value for the density approach, or a more simplistic and lighter design for the level-set approach.

Function	1st eigenfrequency [Hz]	2nd eigenfrequency [Hz]	M_{nd} [%]	Iterations
Density	12.51	61.55	0.28	107
Level-set	12.51	36.13	0.04	159

Table 15: Case study results where every parameter is optimized to achieve the best performance.

(a) Density approach representation.   (b) CSRBF 4 density representation.   (c) CSRBF 4 zero level-set representation.

Figure 28: Results for the second case where every parameter is optimized to achieve the best performance.
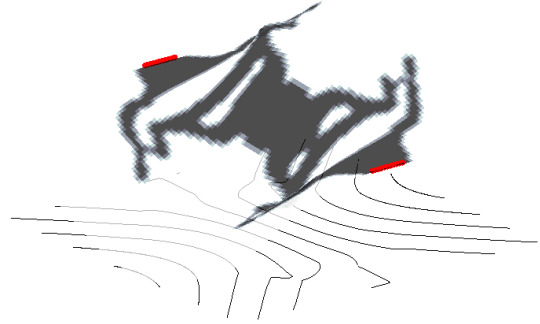
(a) First eigenmode of the density approach.   (b) Second eigenmode of the density approach.
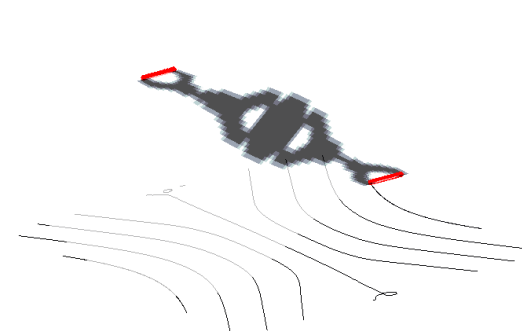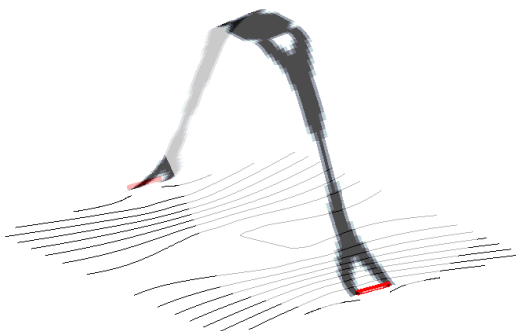
(c) First eigenmode of the level-set approach.   (d) Second eigenmode of the level-set approach.

Figure 29: Eigenmodes of the resulting designs of the density and level-set approach for the second study. The red lines indicate the boundary condition of the plate.
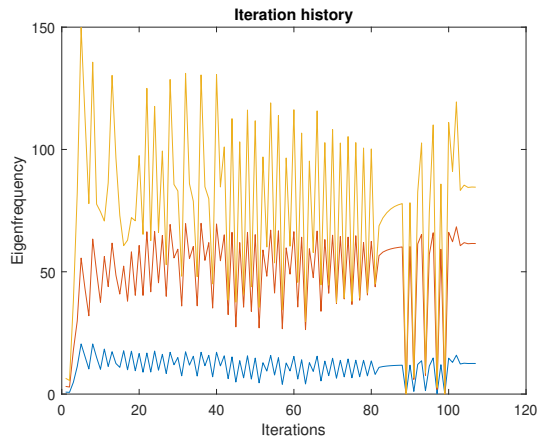
(a) Iteration history of the density optimization run with a filter radius of 2 elements.
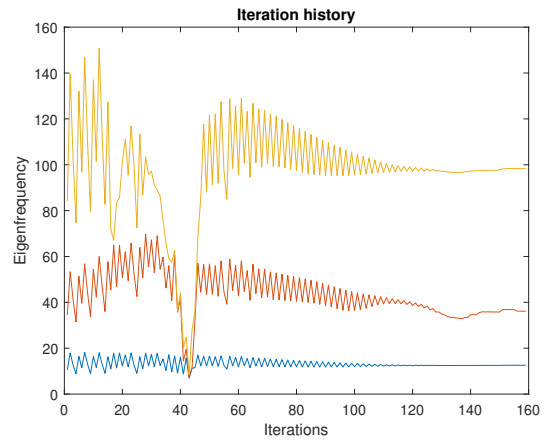
(b) Iteration history of the level-set optimization run with 5 elements for the support radius.

Figure 30: Optimization runs of the density and level-set method for the second study of the Chest Master spring.

8   Conclusion and recommendations

8.1   Conclusions

The set up
This study provides an extensive comparison of the density and level-set approach, which solve various design cases with the use of topology optimization for vibration problems. The main objective of this research is to compare the performance of both approaches and test their applicability in the academic and industrial field. To be able to make a scientifically significant comparison, most of the features of the level-set approach are similar to the density approach. This in turn results in most similarities between the two approaches in terms of parameterization and computation strategy. The density approach uses the modified SIMP method to resolve the occurrence of localized eigenmodes. On top of that, two different filters are incorporated into the density approach to have an additional design representation. The density and level-set approach have common features including material penalization, geometry mapping and using MMA as the update procedure with the use of material parameter sensitivities. However, the level-set approach is parameterized using three different CSRBF. These functions are chosen, as they provide a balance between design detail, convergence rate and memory allocation. To ensure that this research solves scientifically sound problems that are consistent with previous work in the topology optimization of vibrating structures, the selected design cases are based on frequently used benchmark problems in literature. These benchmark cases determine the most optimal settings for each of the density and level-set approach, where after an industrial design case is solved with the use of these settings. The final results of each design case is compared via a set of both qualitative and quantitative criteria. This structured approach highlights the differences in the applied approaches. In general, this thesis shows that the density and level-set approach are both capable of producing useful results in the field of topology optimization for vibration problems. However, there are some pros and cons with the use of each method.

The density approach
The density method is able to produce well-performing designs over all the implemented design cases. Additionally, the mesh size study revealed that a coarse mesh simulation favors the density method slightly more, as it needs less iterations to converge and the results showed a slightly more improved objective function. Furthermore, the density approach has less method specific parameters, making this approach easier to understand and less time consuming to implement. However, the density method is more prone to the occurrence of localized eigenmodes. The localized eigenmodes did not seem to cause any problems during the optimization processes, however it is something to be noted. Thus, the density method is a good all-round method which is accessible in an industrial setting, that does not need much tuning of the method specific parameters to work properly. From an academic viewpoint, the density approach is more easy to implement and a variety of literature is available for extensions of the approach. However, the approach does not always result in the most optimal performance for a given design case.

The level-set approach
The level-set approach slightly outperformed the density approach in most of the design cases. Furthermore, the level-set simulations did not suffer from localized eigenmodes. On the other hand, this approach comprises of more complex method specific parameters such as the support radius or type of CSRBF. However, the design cases revealed that the CSRBF 4 with a support radius of 6 elements produced consistently well performing results. Moreover, the results of the mesh size study reveal that a small mesh size results in a slightly more improved objective function compared to the density approach. For an industrial environment, the level-set approach has a major advantage in that the final design representation can be more easily recreated in a CAD environment. Furthermore, the approach produces well performing designs with the proposed parameters. For further improvements of the results, the level-set approach might take more tuning time of the method specific parameters compared to the density approach. From an academic viewpoint, the level-set approach has the ability to solve more complex vibration problems with more performance.

Industrial design case

Finally, an industrial design case has been optimized with the use of topology optimization to prove its versatility to solve complex problems. In this case a planar spring must have the first eigenfrequency at f_0 = 12.5 Hz and higher eigenfrequencies must be at least twice as high as the first eigenfrequency. The plate used to be manually modified without a clear improvement of the objective function. Two design studies have been evaluated, where one study (study 1) uses the parameters implemented at the comparison of the design cases in Section 5 and another study (study 2) that looks for the ultimate performance. The results of study 1 favored the level-set approach, as the final design of the density representation had a disconnected part. This disconnection of the part resulted in a wrong shape of the first eigenmode. Study 2 revealed that both the density and level-set approach could be used for the application. The differences lied in that the density approach had a higher second order eigenfrequency, whereas the level-set approach has more simple geometric features and a lighter design. This case study illustrates that topology optimization is not a black box design tool that can be applied to any problem without thinking. To get the best out of both methods, tuning of parameters is needed. This tuning will be more effective with more topology optimization knowledge and experience.

Concluding

To conclude, both methods are well-suited to solve a variety of design cases in the field of topology optimization for vibration problems. Key differences of the methods are the ability to obtain a more improved objective function, occurrence of localized eigenmodes, complexity of the applied approach and design representation. On one hand, the density approach is easy to implement and is slightly more favored for a coarse mesh, however it can be more prone to instabilities and a less optimal objective function. On the other hand, the level-set approach can have an improved objective function, has a crisp final design representation and did not encounter local eigenmodes, however the method is more complex to tune the method specific parameters.

8.2 Future research

This thesis can be used as a baseline for future studies on vibration problems. The sheer amount of design cases used in this work can act as reference for newly developed techniques. Additionally, a small part of the code that solves multiplicity is added in Appendix B

- Future work on the current topic (i.e. comparison of topology optimization for vibration problems) should further validate the findings in this thesis with more complicated design cases in combination with a more comprehensive FE analysis. This is most important regarding the performance study of Section 6.6. This study could suffer from a poor FE analysis and only one sample has been tested. Therefore, additional testing may find different results.

- Furthermore, the presented framework uses a level-set approach, which is based on the density method. Although this mapping has most similarities with the density method, there are more mapping methods for the level-set approach (e.g. immersed boundary and conforming discretization) that could outperform the density mapping.

- Moreover, the presented framework has no control over mode shapes. This type of optimization has been investigated by Tsai and Cheng [2013], however the author could not replicate the techniques used in this work. Mode shape optimization is useful for a variety of design cases, where specific positions of the geometry need to contain nodes or anti-nodes. Further investigation of this type of vibration optimization would solve recurrent design cases in industrial environments.

- Finally, the author believes that topology optimization should be more accessible for users in an industrial environment. The tool would give an useful early insight in possible solutions to solve a given design case, which is currently more difficult to realise. To make topology optimization more accessible, it would be convenient that most, if not all, settings should be automatically provided by the program based on the design input. A method like hyperparameter optimization could provide a solution to make the parameters readily available.

9   Bibliography

G. Allaire and F. Jouve. A level-set method for vibration and multiple loads structural optimization. *Computer Methods in Applied Mechanics and Engineering*, 194(30-33 SPEC. ISS.):3269–3290, 2005. ISSN 00457825. doi:10.1016/j.cma.2004.12.018.

G. Allaire, F. Jouve, and A. M. Toader. *Structural optimization using sensitivity analysis and a level-set method*, volume 194. 2004. ISBN 3316933301. doi:10.1016/j.jcp.2003.09.032.

O. Amir, N. Aage, and B. S. Lazarov. On multigrid-CG for efficient topology optimization. *Structural and Multidisciplinary Optimization*, 49(5):815–829, 5 2014. ISSN 1615-147X. doi:10.1007/s00158-013-1015-5. URL http://link.springer.com/10.1007/s00158-013-1015-5.

C. S. Andreasen, M. O. Elingaard, and N. Aage. Level set topology and shape optimization by density methods using cut elements with length scale control. *Structural and Multidisciplinary Optimization*, 62 (2):685–707, 2020. ISSN 16151488. doi:10.1007/s00158-020-02527-1.

K. J. Bathe and F. Brezzi. on the Convergence of a Four-Node Plate Bending Element Based on Mindlin/Reissner Plate Theory and a Mixed Interpolation. 21(March 1984):491–503, 1985. doi:10.1016/b978-0-12-747255-3.50042-3.

R. Behrou, R. Lotfi, J. V. Carstensen, F. Ferrari, and J. K. Guest. Revisiting element removal for density-based structural topology optimization with reintroduction by Heaviside projection. *Computer Methods in Applied Mechanics and Engineering*, 380:113799, 2021. ISSN 00457825. doi:10.1016/j.cma.2021.113799. URL https://doi.org/10.1016/j.cma.2021.113799.

M. P. Bendsøe. Optimal shape design as a material distribution problem. *Structural Optimization*, 1(4): 193–202, 1989. ISSN 09344373. doi:10.1007/BF01650949.

M. P. Bendsøe and O. Sigmund. *Topology Optimization, Theory, Methods, and Applications*. Springer Berlin Heidelberg, Berlin, Heidelberg, 2 edition, 2004. ISBN 978-3-642-07698-5. doi:10.1007/978-3-662-05086-6. URL http://link.springer.com/10.1007/978-3-662-05086-6.

T. E. Bruns and D. A. Tortorelli. Topology optimization of non-linear elastic structures and compliant mechanisms. *Computer Methods in Applied Mechanics and Engineering*, 190(26-27):3443–3459, 3 2001. ISSN 00457825. doi:10.1016/S0045-7825(00)00278-4.

M. D. Buhmann. Radial basis functions. *Acta Numerica*, 9:1–38, 7 2000. ISSN 14740508. doi:10.1017/S0962492900000015. URL https://www.cambridge.org/core/product/identifier/9780511543241/type/book.

R. Courant and D. Hilbert. *Methods of Mathematical Physics*, volume 1. Wiley, 4 2007. ISBN 9783527617210. doi:10.1002/9783527617210. URL https://onlinelibrary.wiley.com/doi/book/10.1002/9783527617210.

M. de Vlieger. How I Developed a Device to Treat My Cystic Fibrosis, 2014. URL https://www.mddionline.com/contract-manufacturing/how-i-developed-device-treat-my-cystic-fibrosis.

Demcon. Demcon, 2021. URL https://demcon.com/.

C. B. Dilgen, S. B. Dilgen, N. Aage, and J. S. Jensen. Topology optimization of acoustic mechanical interaction problems: a comparative review. *Structural and Multidisciplinary Optimization*, 60(2):779–801, 2019. ISSN 16151488. doi:10.1007/s00158-019-02236-4.

J. Du and N. Olhoff. Topological design of freely vibrating continuum structures for maximum values of simple and multiple eigenfrequencies and frequency gaps. *Structural and Multidisciplinary Optimization*, 34(2):91–110, 2007. ISSN 16151488. doi:10.1007/s00158-007-0101-y.

J. K. Guest, J. H. Prévost, and T. Belytschko. Achieving minimum length scale in topology optimization using nodal design variables and projection functions. *International Journal for Numerical Methods in Engineering*, 61(2):238–254, 2004. ISSN 00295981. doi:10.1002/nme.1064.

K. Hassan, E. Ali, and M. Tawfik. Finite elements for the one variable version of mindlin-reissner plate. *Latin American Journal of Solids and Structures*, 17(6):1–18, 2020. ISSN 16797825. doi:10.1590/1679-78256170.

M. F. Heertjes and Y. Vardar. Self-tuning in sliding mode control of high-precision motion systems. *IFAC Proceedings Volumes (IFAC-PapersOnline)*, 46(5):13–19, 2013. ISSN 14746670. doi:10.3182/20130410-3-CN-2034.00019.

M. Huigsloot, M. Langelaar, S. K. Janbahan, and A. Delissen. *Topology optimization involving constrained eigenfrequencies*. PhD thesis, TU Delft, 2018. URL http://resolver.tudelft.nl/uuid:b121092a-4b02-4ec1-8888-c2cbe893094d.

J. S. Jensen and N. L. Pedersen. On maximal eigenfrequency separation in two-material structures: The 1D and 2D scalar cases. *Journal of Sound and Vibration*, 289(4-5):967–986, 2006. ISSN 10958568. doi:10.1016/j.jsv.2005.03.028.

Z. Kang, J. He, L. Shi, and Z. Miao. A method using successive iteration of analysis and design for large-scale topology optimization considering eigenfrequencies. *Computer Methods in Applied Mechanics and Engineering*, 362, 2020. ISSN 00457825. doi:10.1016/j.cma.2020.112847. URL www.sciencedirect.comwww.elsevier.com/locate/cma.

N. H. Kim, T. Dong, D. Weinberg, and J. Dalidd. Generalized optimality criteria method for topology optimization. *Applied Sciences (Switzerland)*, 11(7), 2021. ISSN 20763417. doi:10.3390/app11073175.

Q. Li, O. Sigmund, J. S. Jensen, and N. Aage. Reduced-order methods for dynamic problems in topology optimization: A comparative study. *Computer Methods in Applied Mechanics and Engineering*, 387: 114149, 2021a. ISSN 00457825. doi:10.1016/j.cma.2021.114149. URL https://doi.org/10.1016/j.cma.2021.114149.

Q. Li, Q. Wu, J. Liu, J. He, and S. Liu. Topology optimization of vibrating structures with frequency band constraints. *Structural and Multidisciplinary Optimization*, 63(3):1203–1218, 2021b. ISSN 16151488. doi:10.1007/s00158-020-02753-7.

Z. Li, T. Shi, and Q. Xia. Eliminate localized eigenmodes in level set based topology optimization for the maximization of the first eigenfrequency of vibration. *Advances in Engineering Software*, 107:59–70, 2017. ISSN 18735339. doi:10.1016/j.advengsoft.2016.12.001. URL http://dx.doi.org/10.1016/j.advengsoft.2016.12.001.

J. Liao, G. Huang, X. Chen, Z. Yu, and Q. Huang. A guide-weight criterion-based topology optimization method for maximizing the fundamental eigenfrequency of the continuum structure. *Structural and Multidisciplinary Optimization*, (1992), 2021. ISSN 16151488. doi:10.1007/s00158-021-02971-7.

Z. Luo, L. Tong, M. Y. Wang, and S. Wang. Shape and topology optimization of compliant mechanisms using a parameterization level set method. *Journal of Computational Physics*, 227(1):680–705, 2007. ISSN 10902716. doi:10.1016/j.jcp.2007.08.011.

Z. D. Ma, N. Kikuchi, and I. Hagiwara. Structural topology and shape optimization for a frequency response problem. *Computational Mechanics*, 13(3):157–174, 12 1993. ISSN 0178-7675. doi:10.1007/BF00370133. URL https://link.springer.com/article/10.1007%2FBF00370133http://link.springer.com/10.1007/BF00370133.

Z.-D. Ma, N. Kikuchi, and H.-C. Cheng. Topological design for vibrating structures. *Computer Methods in Applied Mechanics and Engineering*, 121(1-4):259–280, 3 1995. ISSN 00457825. doi:10.1016/0045-7825(94)00714-X. URL https://linkinghub.elsevier.com/retrieve/pii/004578259400714X.

MATLAB. MATLAB R2021b, 2021. URL https://nl.mathworks.com/products/matlab.html.

N. Olhoff. Optimal Structural Design via Bound Formulation and Mathematical Programming. volume 17, pages 255–262. 1989. doi:10.1007/978-3-642-83707-4_32. URL http://link.springer.com/10.1007/978-3-642-83707-4_32.

S. Osher and J. A. Sethian. Fronts propagating with curvature-dependent speed: Algorithms based on Hamilton-Jacobi formulations. *Journal of Computational Physics*, 79(1):12–49, 1988. ISSN 10902716. doi:10.1016/0021-9991(88)90002-2.

N. L. Pedersen. Maximization of eigenvalues using topology optimization. *Structural and Multidisciplinary Optimization*, 20(1):2–11, 2000. ISSN 1615147X. doi:10.1007/s001580050130.

S. Rojas-Labanda and M. Stolpe. Benchmarking optimization solvers for structural topology optimization. *Structural and Multidisciplinary Optimization*, 52(3):527–547, 2015. ISSN 16151488. doi:10.1007/s00158-015-1250-z.

G. I. Rozvany. A critical review of established methods of structural topology optimization. *Structural and Multidisciplinary Optimization*, 37(3):217–237, 2009. ISSN 1615147X. doi:10.1007/s00158-007-0217-0.

G. I. N. Rozvany, M. Zhou, and T. Birker. Generalized shape optimization without homogenization. *Struc-

tural Optimization, 4(3-4):250–252, 1992. ISSN 0934-4373. doi:10.1007/bf01742754.

A. P. Seyranian, E. Lund, and N. Olhoff. Multiple eigenvalues in structural optimization problems. *Structural Optimization*, 8(4):207–227, 1994. ISSN 09344373. doi:10.1007/BF01742705.

O. Sigmund. *Design of Material Structures Using Topology Optimization*. PhD thesis, 1994. URL http://link.springer.com/10.1007/s00158-015-1294-0.

O. Sigmund. On the design of compliant mechanisms using topology optimization. *Mechanics of Structures and Machines*, 25(4):493–524, 1997. ISSN 08905452. doi:10.1080/08905459708945415.

O. Sigmund. Morphology-based black and white filters for topology optimization. *Structural and Multidisciplinary Optimization*, 33(4-5):401–424, 2007. ISSN 1615147X. doi:10.1007/s00158-006-0087-x.

O. Sigmund and K. Maute. Topology optimization approaches: A comparative review. *Structural and Multidisciplinary Optimization*, 48(6):1031–1055, 2013. ISSN 1615147X. doi:10.1007/s00158-013-0978-6.

M. Stolpe and K. Svanberg. An alternative interpolation scheme for minimum compliance topology optimization. *Structural and Multidisciplinary Optimization*, 22(2):116–124, 9 2001. ISSN 1615-147X. doi:10.1007/s001580100129. URL http://link.springer.com/10.1007/s001580100129.

K. Svanberg. The method of moving asymptotes—a new method for structural optimization. *International Journal for Numerical Methods in Engineering*, 24(2):359–373, 2 1987. ISSN 0029-5981. doi:10.1002/nme.1620240207. URL https://onlinelibrary.wiley.com/doi/10.1002/nme.1620240207.

K. Svanberg. MMA and GCMMA – two methods for nonlinear optimization. *Kth*, 1:1–15, 2007.

D. Tcherniak. Topology optimization of resonating structures using SIMP method. *International Journal for Numerical Methods in Engineering*, 54(11):1605–1622, 2002. ISSN 00295981. doi:10.1002/nme.484.

T. D. Tsai and C. C. Cheng. Structural design for desired eigenfrequencies and mode shapes using topology optimization. *Structural and Multidisciplinary Optimization*, 47(5):673–686, 2013. ISSN 1615147X. doi:10.1007/s00158-012-0840-2.

N. P. van Dijk, K. Maute, M. Langelaar, and F. van Keulen. Level-set methods for structural topology optimization: a review. *Structural and Multidisciplinary Optimization*, 48(3):437–472, 9 2013. ISSN 1615-147X. doi:10.1007/s00158-013-0912-y. URL http://link.springer.com/10.1007/s00158-013-0912-y.

C. H. Villanueva and K. Maute. Density and level set-XFEM schemes for topology optimization of 3-D structures. *Computational Mechanics*, 54(1):133–150, 2014. ISSN 01787675. doi:10.1007/s00466-014-1027-z.

C. Wang, Z. Zhao, M. Zhou, O. Sigmund, and X. S. Zhang. *A comprehensive review of educational articles on structural and multidisciplinary optimization*, volume 64. Springer Berlin Heidelberg, 2021. ISBN 0123456789. doi:10.1007/s00158-021-03050-7. URL https://doi.org/10.1007/s00158-021-03050-7.

F. Wang, B. S. Lazarov, and O. Sigmund. On projection methods, convergence and robust formulations in topology optimization. *Structural and Multidisciplinary Optimization*, 43(6):767–784, 2011. ISSN 1615147X. doi:10.1007/s00158-010-0602-y.

J. Wang, M. Zhang, Y. Zhu, K. Yang, X. Li, L. Wang, J. Hu, and C. Hu. Integrated optimization of 3D structural topology and actuator configuration for vibration control in ultra-precision motion systems. *Structural and Multidisciplinary Optimization*, 60(3):909–925, 9 2019. ISSN 1615-147X. doi:10.1007/s00158-019-02244-4. URL http://link.springer.com/10.1007/s00158-019-02244-4.

M. Y. Wang, X. Dai, P. Tang, X. Cheng, and M. Wu. A variational binary level set method for structural topology optimization. *Communications in Computational Physics*, 13(5):1292–1308, 2003. ISSN 19917120. doi:10.4208/cicp.160911.110512a.

P. Wei, Z. Li, X. Li, and M. Y. Wang. An 88-line MATLAB code for the parameterized level set method based topology optimization using radial basis functions. *Structural and Multidisciplinary Optimization*, 58(2):831–849, 2018. ISSN 16151488. doi:10.1007/s00158-018-1904-8.

P. Wei, W. Wang, Y. Yang, and M. Y. Wang. Level set band method: A combination of density-based and level set methods for the topology optimization of continuums. *Frontiers of Mechanical Engineering*, 15(3):390–405, 2020. ISSN 20950241. doi:10.1007/s11465-020-0588-0.

H. Wendland. Piecewise polynomial, positive definite and compactly supported radial functions of minimal degree. *Advances in Computational Mathematics*, 4(1):389–396, 1995. ISSN 10197168.

doi:10.1007/BF02123482.

W. H. Wittrick. Rates of Change of Eigenvalues, With Reference to Buckling and Vibration Problems. *The Journal of the Royal Aeronautical Society*, 66(621):590–591, 9 1962. ISSN 0368-3931. doi:10.1017/s0368393100077385. URL https://www.cambridge.org/core/product/identifier/S0368393100077385/type/journal_article.

H. Xia, Z. Qiu, and L. Wang. Reliability-based topology optimization for freely vibrating continuum structures with unknown-but-bounded uncertainties. *Structural and Multidisciplinary Optimization*, 63(6): 2751–2770, 2021. ISSN 16151488. doi:10.1007/s00158-020-02834-7.

S. Xu, Y. Cai, and G. Cheng. Volume preserving nonlinear density filter based on heaviside functions. *Structural and Multidisciplinary Optimization*, 41(4):495–505, 2010. ISSN 1615147X. doi:10.1007/s00158-009-0452-7.

G. H. Yoon. Maximizing the fundamental eigenfrequency of geometrically nonlinear structures by topology optimization based on element connectivity parameterization. *Computers and Structures*, 88(1-2):120–133, 2010. ISSN 00457949. doi:10.1016/j.compstruc.2009.07.006. URL http://dx.doi.org/10.1016/j.compstruc.2009.07.006.

S. Zargham, T. A. Ward, R. Ramli, and I. A. Badruddin. Topology optimization: a review for structural designs under vibration problems. *Structural and Multidisciplinary Optimization*, 53(6):1157–1177, 2016. ISSN 16151488. doi:10.1007/s00158-015-1370-5. URL http://dx.doi.org/10.1007/s00158-015-1370-5.

P. Zhou, J. Du, and Z. Lü. Topology optimization of freely vibrating continuum structures based on nonsmooth optimization. *Structural and Multidisciplinary Optimization*, 56(3):603–618, 2017. ISSN 16151488. doi:10.1007/s00158-017-1677-5. URL http://dx.doi.org/10.1007/s00158-017-1677-5.

J. Zhu, W. Zhang, and P. Beckers. Integrated layout design of multi-component system. *International Journal for Numerical Methods in Engineering*, 78(6):631–651, 5 2009. ISSN 00295981. doi:10.1002/nme.2499. URL https://onlinelibrary.wiley.com/doi/10.1002/nme.2499.

K. T. Zuo, L. P. Chen, Y. Q. Zhang, and J. Yang. Study of key algorithms in topology optimization. *International Journal of Advanced Manufacturing Technology*, 32(7-8):787–796, 2007. ISSN 02683768. doi:10.1007/s00170-005-0387-0.

A   Overall evaluation of best results

From the results it was found that the Heaviside filter and the CSRBF 4 produced the overall best result from the design cases. This section provides a more clear overview of these obtained results from Section 6.

Method	Optimized result	ω [rad/s]	M_{nd} [%]	Iterations
Section 6.1				
Density		173.2	1.37	46
Level-set (VF)		174.5	0.80	84
Zero level-set				
Section 6.2				
Density		9.53	3.52	35
Level-set (VF)		8.90	1.41	58
Zero level-set				
Section 6.3				
Density		304.7	0.26	64
Level-set (VF)		301.9	2.72	88
Zero level-set				

Table 16: Results of the selected best performing method for the 2D in plane cases. The selected methods are the Heaviside filer for the density approach and the CSRBF 4 for the level-set approach. The abbreviation (VF) refers to the Ersatz volume fraction of the level-set approach.
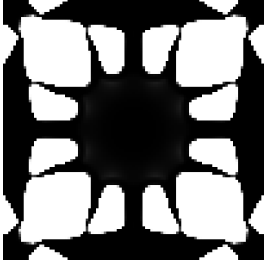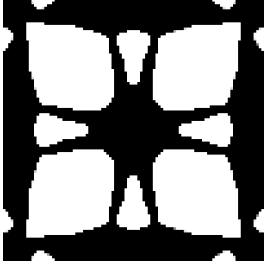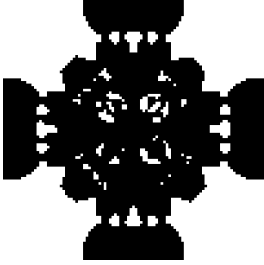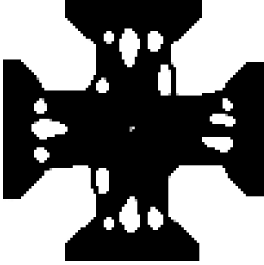
Method	Optimized result	ω [rad/s]	M_{nd} [%]	Iterations
Section 6.4				
Density		75.6	2.93	43
Level-set (VF)		76.6	0.15	41
Section 6.5				
Density		650.0	0.01	65
Level-set (VF)		756.7	0.17	62

Table 17: Results of the selected best performing method for the 3D plate cases. The selected methods are the Heaviside filer for the density approach and the CSRBF 4 for the level-set approach. The abbreviation (VF) refers to the Ersatz volume fraction of the level-set approach.

B   Multiplicity matlab code

This section shows a function of the matlab code, where a multiplicity condition of two eigenfrequencies occurs. The code is meant to be used for future research.

```matlab
function [dc] = Sensitivites_double(k,phi,penal,E0,Emin,xPhys,nelx,nely,...
    KE,ME,labda,edofMat)
% This function solves the sensitivities for a multiple eigenvalue of two
% adjacent eigenvalues. For an extension to three or more multiple
% eigenvalues the [g] matrix should be expanded accordingly
%
%        k = lowest eigenmode of multiple eigenvalue
%      phi = eigenmodes corresponding to the multiple eigenvalue
%    penal = the penalty value of the modified simp
%       E0 = Young's modulus
%     Emin = minimal Young's modulus value
%    xPhys = Element density
%     nelx = amount of elements in x-direction
%     nely = amount of elements in y-direction
%       KE = elemental stiffness matrix
%       ME = elemental mass matrix
%    labda = eigenvalue of the multiple eigenvalue
% edofMat = the element node numbering
%% sensitivity calculation for adjacent frequencies
for k = k
  for i = 1:nelx
      for j = 1:nely
        %%% Element numbering
        el = (i-1)*nely+j;
        %%% Sensitivities of the elemental matrices
        delc = (penal*(E0-Emin)*xPhys(j,i).^(penal-1)*KE - labda(k)*ME);

        %%% Setup the G matrix
        g11(j,i) = phi([edofMat(el,:)],k)'  * delc* phi([edofMat(el,:)],k);
        g12(j,i) = phi([edofMat(el,:)],k)'  * delc* phi([edofMat(el,:)],k+1);
        g22(j,i) = phi([edofMat(el,:)],k+1)'* delc* phi([edofMat(el,:)],k+1);
        A        = [g11(j,i), g12(j,i); g12(j,i), g22(j,i)];
        [VV,WW] = eigs(A);
        WW      = diag(WW);

        %%% new sensitivities matrix
        for o = k:k+1
            dc(j,i,o)= WW(o+1-k);
        end
      end
    end
    gg(:,:,1) = g11;
    gg(:,:,2) = g22;

    %%% check if off-diagonal terms are zero
    if abs(sum(sum(g12))) < 1e-4
        for o = k:k+1
            dc(:,:,o) = gg(:,:,o+1-k);
        end
        fprintf('No multiplicity %g.\n');
    else
        fprintf('Double Multiplicity %g.\n');
    end
end
```

C   FEM check

It is important to validate the implemented FEM to have representative results. The elements of the 8 DOF 4 node quadrilateral plane stress elements and the 12 DOF 3D 4 node quadrilateral Mindlin-Reissner elements have been checked via COMSOL and the paper of Du and Olhoff [2007]. The simply supported beam of Figure 14.1 is used with a density of $\rho = 1$, a Young's modulus of $E = 10^7$ MPa, a Poisson's ratio of $\nu = 0.3$, 240x30 quadrilateral plane stress elements and a dimension of 8x1 m. The results are shown in Table 18 and the resulting first eigenmode in Figure 31.

Model	Eigenfrequency [rad/s]
COMSOL	68.1537
Du and Olhoff [2007]	68.7
Current work	68.3209

Table 18: Eigenfrequency results for validation of plane stress FE.

(a) Comsol FEM check in plane

(b) Matlab FEM check in plane
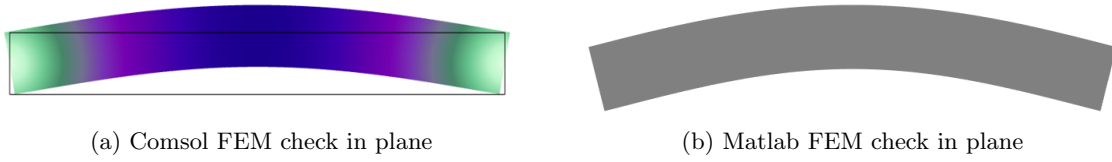
Figure 31: 2 Figures side by side

Furthermore, the out of plane Mindlin-Reissner elements are only validated via COMSOL. These results are shown in Table 19 and visual results in Figure 32.

Model	Eigenfrequency [rad/s]
COMSOL	106.1544
Current work	106.1518

Table 19: Eigenfrequency results for validation of the Mindlin-Reissner FE.

(a) Comsol FEM check out of plane

(b) Matlab FEM check out of plane
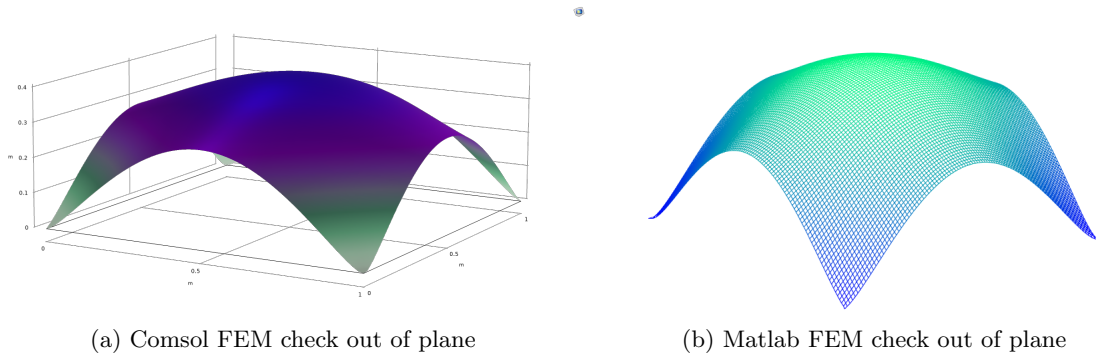
Figure 32: 2 Figures side by side

D   Validating results with literature

This section validates the obtained results of the design case of the beam with simply supported ends, which is the boundary condition of Figure 14.1. The results from Du and Olhoff [2007] are used to compare with. The parameter settings used in this work are different from that in the work of Du and Olhoff. However, it gives in indication in the corectness of the implemented approach.

Figure 33: Results for the simply supported beam from Du and Olhoff [2007] with the use of a sensitivity filter.

Figure 34: Results for the sensitivity filter with a filter radius of 3 elements.

Figure 35: Level-set results of the CSRBF 4 and 6 elements support radius.

E   Filter and support radii study

This section represents the results for different filter and support radii and their corresponding results. The study shows the influence of the filter and support radius for the design representation. All of these examples have the objective function of maximizing the fundamental eigenfrequency for the boundary condition of Figure 14.1 and the boundary condition of Figure 14.4 are used. All the parameters are fixed, except for the filter and support radii. The density approach uses the filter radii of $r_{min} = [1.5,2,2.5,3,4]$ elements for all examples. The level-set approach uses R = [2,3,4,5,6,7,8] elements for the beam example and R = [3,4,5,6,7,8] elements for the plate example.

The results of this study can be seen in Table 20 till 23. The results show the objective function, measure of non-discreteness and amount of iterations until convergence. The results of these studies are not related with the results obtained in section 8.

Elements	Optimized result	ω	M_{nd}
	Sensitivity filter		
1.5		174.2	5.73
2		173.9	3.66
2.5		172.7	5.77
3		172.2	4.53
4		171.1	5.91
	Heaviside filter		
1.5		174.2	0.24
2		173.8	0.47
2.5		174.3	0.92
3		173.5	1.64
4		172.5	172.5

Table 20: Results for the beam like example. The density method and different filter radii for the sensitivity and Heaviside filter are used. The corresponding values for ω [rad/s] and M_{nd} is [%] is behind the results.

Elements	Density representation	Zero level-set	ω	M_{nd}
	CSRBF 2			
2			161.05	17.57
3			181.53	1.71
4			180.42	1.89
5			179.83	1.78
6			180.85	1.66
7			182.61	0.97
8			182.00	0.81
	CSRBF 4			
2			183.29	1.08
3			185.18	0.27
4			184.74	0.35
5			185.18	0.39
6			180.59	0.38
7			182.63	0.25
8			180.95	0.10
	CSRBF 6			
2			171.18	11.54
3			182.54	1.20
4			184.78	0.47
5			182.72	0.82
6			173.27	1.06
7			182.83	0.95
8			183.68	0.55

Table 21: Results for the beam like example of the level-set method and different radii for the CSRBF. The corresponding values for ω [rad/s] and M_{nd} is [%] is behind the results.
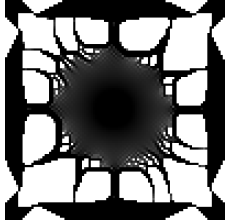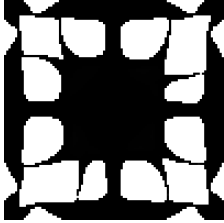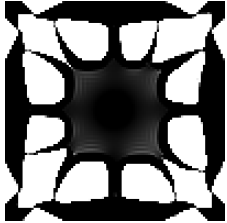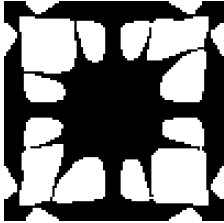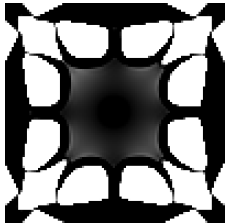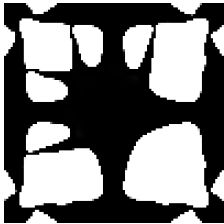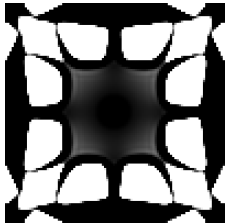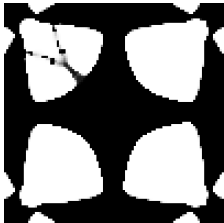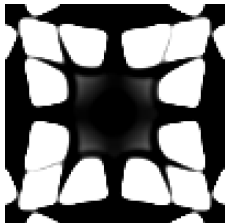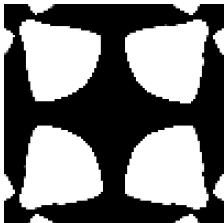
Elements	Sensitivity filter	Results	Heaviside filter	Results
1.5		ω=74.54 M_{nd}=9.86		ω=75.03 M_{nd}=0.57
2		ω=75.38 M_{nd}=6.30		ω=72.09 M_{nd}=0.14
2.5		ω=74.85 M_{nd}=9.96		ω=75.17 M_{nd}=0.64
3		ω=74.93 M_{nd}=9.97		ω75.04 M_{nd}=1.38
4		ω=74.74 M_{nd}=9.12		ω=75.60 M_{nd}=0.65

Table 22: Results for the density method and different filter radii for the plate like example. The corresponding values for ω [rad/s] and M_{nd} is [%] is behind the results.
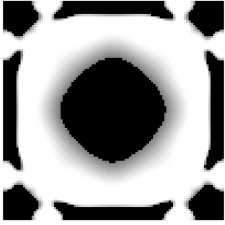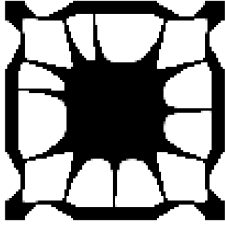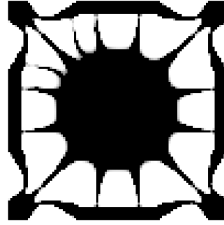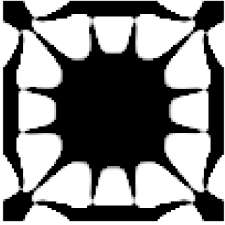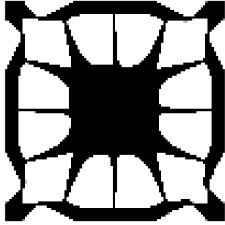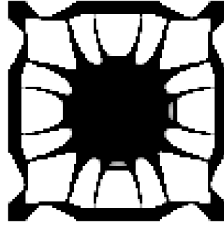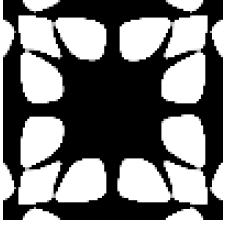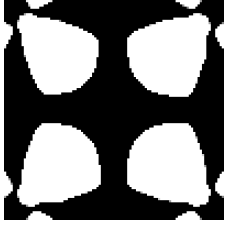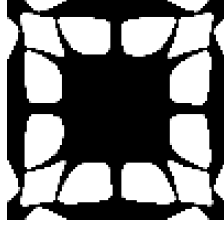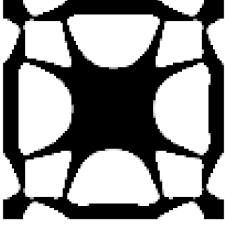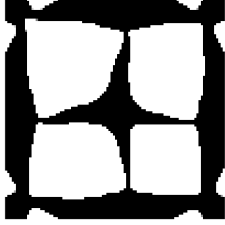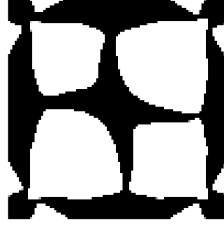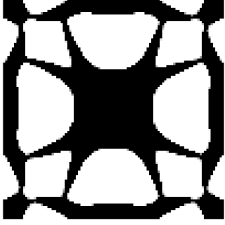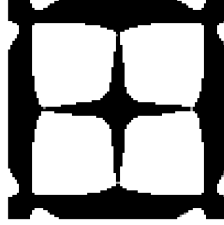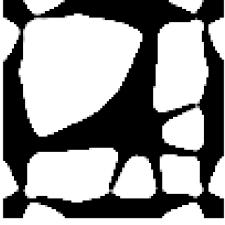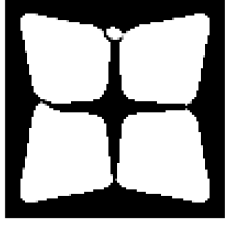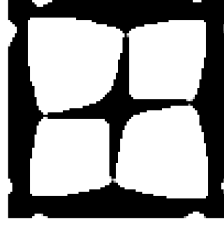
Elements	CSRBF 2	Results	CSRBF 4	Results	CSRBF 6	Results
3		ω=0.06 M_{nd}=15.03		ω=72.91 M_{nd}=0.38		ω=70.94 M_{nd}=2.08
4		ω=70.99 M_{nd}=3.92		ω=73.60 M_{nd}=0.18		ω=72.15 M_{nd}=1.12
5		ω=73.15 M_{nd}=1.65		ω=75.41 M_{nd}=0.06		ω=73.63 M_{nd}=0.26
6		ω=73.39 M_{nd}=1.61		ω=76.15 M_{nd}=0.08		ω=75.71 M_{nd}=0.16
7		ω=73.65 M_{nd}=1.01		ω=76.63 M_{nd}=0.11		ω=76.71 M_{nd}=0.09
8		ω=73.73 M_{nd}=1.09		ω=76.16 M_{nd}=0.22		ω=76.46 M_{nd}=0.14

Table 23: Results for the level-set method and different filter radii for the different CSRBF for the plate like example. The corresponding values for ω [rad/s] and M_{nd} is [%] is behind the results. Only the density representation of the level-set function is shown.